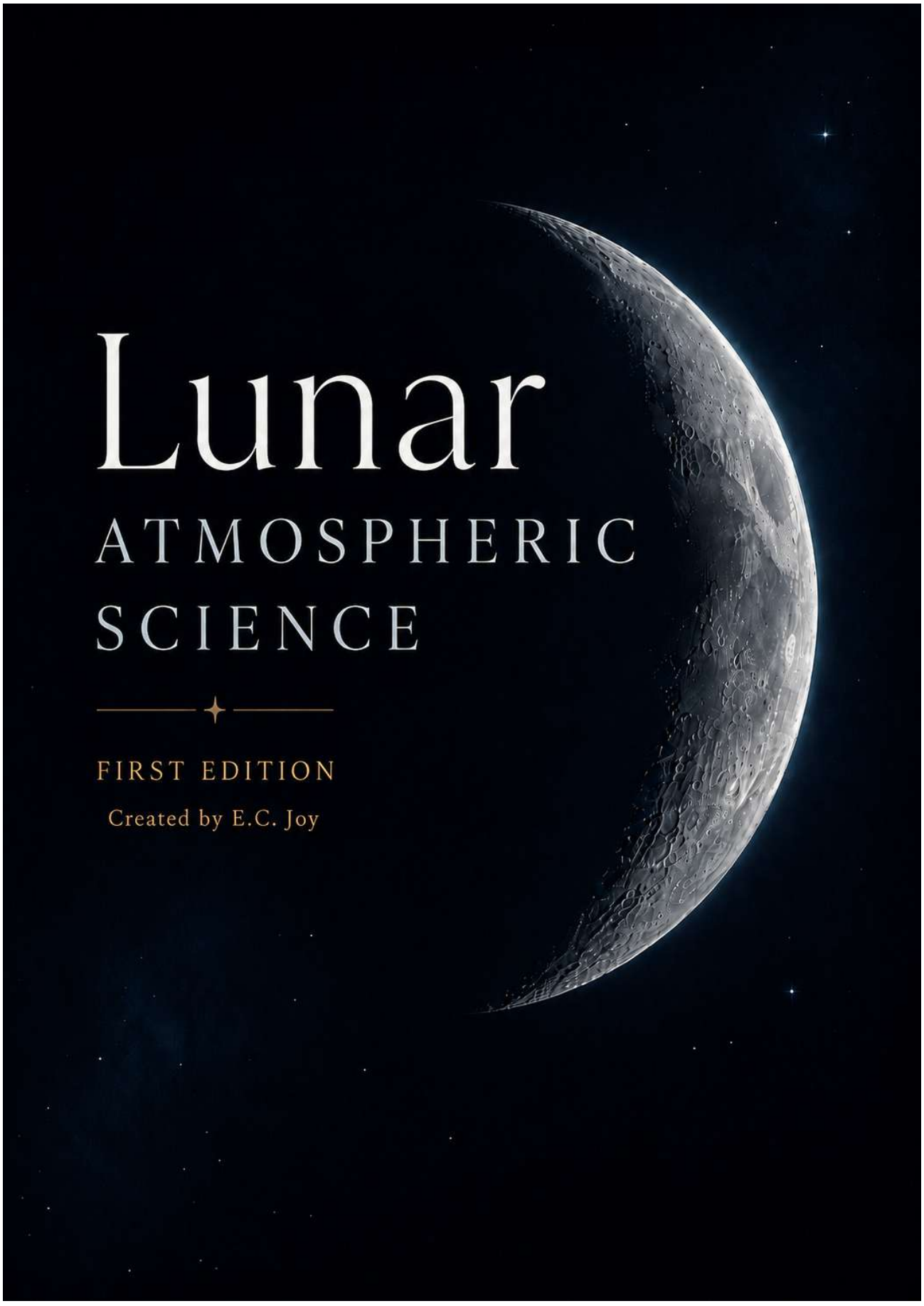
Lunar
ATMOSPHERIC
SCIENCE
FIRST EDITION
Created by E.C. Joy

TABLE OF CONTENTS

Part 1 — Chart / Quick Reference 2
Part 2 — Introduction to Lunar Atmospheric Science 5
Part 3 — The Lunar Environment: Physical Context 7
Part 4 — Nature of the Lunar Atmosphere: Surface-Bounded Exosphere 9
Part 5 — Composition of the Lunar Exosphere 11
Part 6 — Structure: Density, Pressure, Temperature, and Vertical Profiles 13
Part 7 — Sources of Atmospheric Constituents 15
Part 8 — Loss Processes and Sinks 17
Part 9 — Surface–Exosphere Interactions 19
Part 10 — Dynamics and Transport 21
Part 11 — Temporal Variability 23
Part 12 — Plasma Environment and Lunar Ionosphere 25
Part 13 — Dust–Exosphere Coupling 27
Part 14 — Observational Techniques and Key Datasets 28
Part 15 — Comparative Planetology: The Lunar Exosphere in Context 30
Part 16 — Applications to Human Exploration and Future Science 31
Part 17 — Open Questions and Frontiers 32
Part 18 — Suggested Further Reading and Key Resources 34
Appendix A — Equation Derivations and Modeling Foundations 36

LUNAR ATMOSPHERIC SCIENCE

Notes for Meteorology Students & Professionals

Part 1 — Chart / Quick Reference

This section collects the essential numerical values, units, and equations used throughout Lunar Atmospheric Science. Values are approximate or representative; densities, source rates, effective temperatures, and lifetimes vary strongly with species, local solar time, latitude, solar activity, and the adopted model. Use primary data and explicitly stated assumptions for quantitative work.

1. Lunar Physical Constants (Atmosphere-Relevant)

Quantity	Value	Notes / comparison
Mean radius (*R*)	1737.4 km	Volumetric mean
Mass (*M*)	7.346×10^{22} kg	≈ 0.0123 times Earth's mass
Surface gravity (*g*)	1.62 m s^{-2}	≈ 0.1654 times Earth's surface gravity
Escape velocity (v_{esc})	2.38 km s^{-1}	Surface value
Standard gravitational parameter ($\mu = GM$)	≈ 4902.8 km^3 s^{-2}	*G* = gravitational constant; *M* = lunar mass
Sidereal rotation period	27.321661 days	Spin–orbit locked
Synodic month	29.530589 days	Full diurnal cycle length
Axial tilt (obliquity)	≈ 1.54°	Small obliquity plus polar topography permits permanently shadowed regions (PSRs)
Bond albedo	≈ 0.11	
Solar irradiance at Moon	1361 W m^{-2}	Same as at Earth

2. Atmospheric Mass, Pressure, and Density

Total atmospheric inventory: a legacy order-of-magnitude estimate is roughly 10–25 metric tonnes for the native neutral exosphere. This is not a continuously measured global mass and can vary with the species inventory and activity level.

Equivalent surface pressure: order 10^{-10}–10^{-9} Pa; the traditional benchmark 3×10^{-15} bar equals 3×10^{-10} Pa. This is a global statistical equivalent or a velocity-moment pressure for a specified population—not a terrestrial, horizontally equilibrated pressure field.

Typical Surface Number Densities

(Highly variable with local time; values from LADEE, LACE, and related observations/models)

Species	Typical density (cm^{-3})	Notes
He	5×10^3 – 6.5×10^4	Peaks around 1–2 a.m. local time; non-condensable
Ne	10^3 – 2×10^4	Noncondensable; pre-dawn maximum from ballistic redistribution
^{40}Ar	2×10^4 – 10^5	Radiogenic; cold-surface adsorption/trapping; maximum near sunrise
Na	~30–70 (column ~10^9–10^{10} cm^{-2})	Hot component; remote sensing

Species	Typical density (cm^{-3})	Notes
K	Lower than Na (column ~10^8 cm^{-2})	Similar behavior to Na
H_2	Variable; tied to solar-wind flux	Detected by LRO/LAMP; source partition remains uncertain
Other volatiles/refractories	Trace, upper limits, or uncertain	Volatile channels may be contamination-limited

During extreme solar-wind events, measured total dayside exospheric number density and pressure can rise by more than an order of magnitude. Interpreting individual refractory-species enhancements requires mass-channel and source-model constraints.

3. Temperature Extremes

- **Equatorial surface:** daytime maximum ≈ 390–400 K; nighttime minimum ≈ 90–100 K.
- **Polar regions (sunlit slopes):** lower daytime maxima; strong seasonal modulation.
- **Permanently Shadowed Regions (PSRs):** routinely < 110 K; many locations 20–50 K; some of the coldest measured surfaces in the inner Solar System (historically reported values approaching or below ~25 K in specific craters such as Hermite).
- **Effective exospheric temperatures:** thermal components track surface temperature; non-thermal components (sputtering, impact vaporization, PSD) commonly 1000–9000 K (especially for Na), producing large scale heights.

4. Key Equations

Scale Height

(Local isothermal, constant-g limit. H is an e-folding length for an ideal thermal population; it does not imply continuum-fluid behavior.)

$$H = kT / (m\,g)$$

where k is Boltzmann's constant, T is the kinetic or source temperature assigned to that population, m is particle mass, and g is local gravitational acceleration.

Jeans Escape Parameter

(Evaluated at radius r)

$$\lambda(r) = GMm / (kTr) = v_{es}c^2 / v_{mp}^2;\ \text{locally, } \lambda \approx r/H$$

where $v_{mp} = \sqrt{(2kT/m)}$ is the most-probable Maxwellian speed. Escape is exponentially suppressed as λ grows; there is no universal threshold at λ = 15. Values near 2–3 imply a large escaping tail, whereas values of 10–20 can still matter over long times if the species is continually resupplied.

Jeans Escape Flux

(Thermal evaporation at the exobase)

$$\Phi_J = (n\,v_{mp} / 2\sqrt{\pi})\,(1 + \lambda)\,e\text{^}(-\lambda)$$

This is the upward flux from an ideal isotropic Maxwellian at a conventional exobase. At the lunar surface, the outgoing distribution is a half-space, flux-weighted distribution and the result must be combined with source, accommodation, sticking, and return-trajectory physics.

Ballistic Trajectory (Constant-g Approximation)

- Time of flight (round-trip hop): $t_D = 2\,v_z / g$
  - Maximum height: $z_max = v_z^2 / (2\,g)$

- Vertical velocity vs. height: $v_z(z) = \sqrt{(v_{z0}^2 - 2 g z)}$

For point-mass gravity, use the exact specific orbital energy $\mathcal{E} = v^2/2 - GM/r$ and angular momentum; $\mathcal{E} < 0$ gives a bound conic and $\mathcal{E} \geq 0$ gives escape. Numerical integration is required when adding nonspherical gravity, topography, radiation pressure, plasma forces, or time-dependent boundaries.

Chamberlain-Type Density Relation for Ballistic Particles

$$n(r) = n(r_0) \exp[\lambda(r) - \lambda_0] \cdot Z(r)/Z(r_0), \quad Z = \zeta_{bal} + \zeta_{esc} + \zeta_{sat}$$

The exponential is the full-Maxwellian barometric factor; the Chamberlain partition functions retain only velocity-space trajectories that are actually populated. Ballistic trajectories return to the lower boundary, escaping trajectories are unbound, and satellite trajectories are bound but do not intersect the lower boundary. For a native surface-launched lunar population, ζ_sat is normally zero unless an external process populates such orbits. Full derivation: Appendix A.

Non-Condensable Gas Equilibrium (Hodges & Johnson Type)

For an ideal noncondensable species in steady, source-free, sink-free, fully accommodated ballistic transport over a slowly varying surface temperature:

$$n_s T_s^{(5/2)} \approx \text{constant} \quad \text{(Hodges–Johnson diffusion limit; not a universal equation of state)}$$

5. Useful Conversions and Scales

- 1 $cm^{-3} \approx 10^6$ m^{-3}
- 1 Pa ≈ 10^{-5} bar ≈ 9.87 × 10^{-6} atm
- Lunar day ≈ 29.53 Earth days (full diurnal cycle)
- Local constant-g thermal scale heights at 100 K and 400 K are approximately: He 128 and 513 km; Ne 25 and 102 km; Ar 13 and 51 km; and Na 22 and 89 km. Curvature becomes important when H is not small compared with the lunar radius.
- Hot sodium populations are often fitted with apparent scale heights of roughly 500–2000 km, but a non-Maxwellian source distribution need not possess a single physical temperature or exponential scale height.
- At quiet-time densities, neutral mean free paths are normally far larger than the relevant vertical scale and commonly comparable to or greater than the lunar radius. The exact value depends on species, cross section, and collision energy.

6. Notes for Meteorologists

- **The lunar "atmosphere" is a surface-bounded exosphere:** particles follow independent ballistic trajectories under gravity with negligible collisions.
- **Classical hydrostatic balance, fluid dynamics, and continuum thermodynamics do not apply** in the usual terrestrial sense.
- **Diurnal temperature swing (~300 K at equator) and the extreme cold of PSRs** dominate source/sink behavior via adsorption, desorption, and cold trapping.
- **Solar-wind implantation, radiogenic release, photon-driven release, impacts, and sputtering replenish different species against escape, photoionization, and surface sequestration; no single source or lifetime describes the whole exosphere.**

The equations in this chart are derived and their assumptions tested in Appendix A. Later sections use these reference values unless a species-specific observation or model is stated explicitly.

Part 2 — Introduction to Lunar Atmospheric Science

Motivation for Meteorologists

Most meteorologists spend their careers working within the dense, collisional, fluid-dynamic regime of Earth's atmosphere. The lunar environment sits at the opposite extreme: a collisionless, surface-bounded exosphere whose particles travel on individual ballistic trajectories under gravity, with essentially no mutual collisions. Studying this regime forces a return to first principles—kinetic theory, ballistic transport, surface–gas interactions, thermal and non-thermal escape, and the direct coupling of a neutral gas to the surrounding space plasma environment.

Several practical and scientific motivations make the lunar atmosphere especially relevant:

- It is the purest accessible example of a surface-bounded exosphere in the Solar System. Concepts that appear only at the extreme upper boundary of Earth's atmosphere (the terrestrial exosphere) dominate the entire lunar "atmosphere."
- Relevant timescales span an enormous range: seconds-to-hours for individual hops and prompt loss, days for some fitted exospheric responses, months for some photoionization lifetimes, and geologic intervals for storage in stable cold traps. The system is nevertheless highly responsive to solar activity, meteoroid flux, and spacecraft contamination.
- Polar cold traps and the transport of water and other volatiles provide an extreme analog to terrestrial polar processes and to the sequestration of volatiles on other airless bodies.
- With sustained human activity returning to the Moon (Artemis and related programs), the native exosphere will be repeatedly perturbed by lander exhaust, rover operations, and habitat outgassing. Understanding the baseline state is a prerequisite for interpreting any changes.

In short, the lunar atmosphere is not a curiosity; it is a limiting case that sharpens intuition about atmospheric physics in general.

Historical Overview

Pre-Apollo observations mostly established upper limits. Apollo cold-cathode gauges and ion instruments provided early evidence for a tenuous near-surface environment, but contamination and mass-channel interpretation complicated several measurements. Apollo 17's Lunar Atmospheric Composition Experiment (LACE) supplied the first definitive in-situ neutral-composition measurements and quantitative diurnal curves for ^{4}He and ^{40}Ar. SIDE detections at m/q ≈ 20–28 and 40–44 were early ion measurements with non-unique species assignments, not standalone proof of corresponding neutral densities. Apollo 15 and 16 alpha-particle spectrometers detected spatially variable ^{222}Rn and ^{210}Po signals, including activity near Aristarchus, supporting localized radiogenic release.

After the end of Apollo funding, the field largely stagnated until the late 1980s, when ground-based observers detected sodium and potassium resonance emissions. These alkali metals, although present only at tens of atoms per cubic centimeter, produce optically bright lines that can be mapped from Earth. The discovery of the lunar sodium "tail" and its variation with solar activity reopened the subject.

A major leap occurred with the Lunar Atmosphere and Dust Environment Explorer (LADEE) mission (2013–2014). LADEE's Neutral Mass Spectrometer provided systematic in-situ measurements of He, Ne, and Ar and searches or constraints for other mass channels, while its Ultraviolet–Visible Spectrometer remotely measured Na and K. Complementary data from LRO/LAMP, Kaguya, Chandrayaan, ARTEMIS, and later Chinese and Indian missions have continued to refine the picture. Isotopic studies of Apollo soils have more recently constrained the relative long-term contributions of micrometeoroid impact vaporization versus solar-wind sputtering.

Scope of the Field and Differences from Classical Meteorology

Lunar atmospheric science is the study of the sources, sinks, composition, structure, dynamics, and plasma interactions of the Moon's surface-bounded exosphere, together with the coupled dust and plasma environment that surrounds it.

The differences from classical terrestrial meteorology are fundamental:

Aspect	Earth	Moon
Collisional regime	Collisional (Knudsen number $\ll 1$) throughout the bulk atmosphere	Collisionless almost everywhere (mean free path $\gg$ scale height)
Governing equations	Navier–Stokes / hydrostatic balance	Individual ballistic trajectories + surface interaction physics
Vertical structure	Distinct troposphere, stratosphere, mesosphere, thermosphere, exosphere	Essentially a single surface-bounded exosphere
Energy transport	Radiation + convection + conduction	Radiation + ballistic particle transport + direct surface heating
Diurnal range	Typically tens of kelvin	~300 K at the equator; extreme polar cold traps
Magnetic field	Global dipole that largely shields the atmosphere	No global field; only localized crustal fields

Consequently, many familiar meteorological concepts (geostrophic balance, baroclinic instability, Hadley cells, etc.) have no direct counterpart. In their place appear ballistic hop statistics, adsorption/desorption kinetics, photon-stimulated desorption, solar-wind sputtering yields, and photoionization + pickup-ion loss.

Relationship to Broader Planetary Science and Space Physics

The lunar exosphere is the nearest well-observed example of a surface-bounded exosphere. Related collisionless atmospheres occur at Mercury, icy satellites, and small bodies, although their dominant species and plasma environments differ. The Moon also provides a plasma laboratory: the solar wind strikes the surface, forms a wake, interacts with crustal magnetic anomalies, and acquires lunar pickup ions produced from the neutral exosphere.

Finally, because the lunar atmosphere is so tenuous, even modest spacecraft activity can dominate the local gas density. This makes the Moon a unique testbed for assessing anthropogenic effects on planetary atmospheres—an issue that will grow in importance as exploration expands.

This introduction is intended to orient the reader and to establish the physical context before the more detailed chapters that follow.

Part 3 — The Lunar Environment: Physical Context

Understanding the lunar atmosphere requires first understanding the physical environment that creates and controls it. Unlike Earth, where the atmosphere is largely self-contained and buffered by a massive fluid reservoir, the lunar exosphere is continuously generated and destroyed by interactions between the surface, solar radiation, the solar wind, and micrometeoroids. The properties of the Moon itself therefore set the boundary conditions for every atmospheric process discussed in later chapters.

Gravity, Size, and Orbital Parameters

The Moon's mean radius is 1737.4 km and its mass is 7.346×10^{22} kg—approximately 1/81 the mass of Earth. Surface gravity is only 1.62 m s^{-2} (0.1654 $g_{\oplus}$), and the surface escape velocity is 2.38 km s^{-1}. These low values have two immediate consequences for the atmosphere:

- At 400 K, the most-probable speed of atomic hydrogen is comparable to or greater than lunar escape speed; helium's is lower but its Maxwellian tail and source-energy distribution still permit substantial gravitational loss. Thermal escape is therefore most important for the lightest species and is highly temperature dependent.
- Even modest non-thermal energies imparted by sputtering or impact vaporization can place particles on escape trajectories.

The Moon is tidally locked to Earth (sidereal rotation period 27.321661 days). The synodic month—the time from new Moon to new Moon as seen from Earth—is 29.530589 days and defines the full diurnal cycle experienced by any point on the lunar surface. The small axial tilt relative to the ecliptic (≈ 1.54°), together with polar topography, permits permanently shadowed regions (PSRs) near the poles and allows seasonal modulation of polar illumination.

Surface Properties: Regolith, Thermal Inertia, Albedo, and Topography

The lunar surface is covered by impact-generated regolith. Grain sizes in the upper centimeters span micrometers to millimeters, and the fines are highly porous. Diviner-based thermophysical models use a bulk density near 1.1 g cm^{-3} at the immediate surface that rises toward about 1.8 g cm^{-3} by ~1 m depth; sample-scale and site-specific values vary. Low thermal inertia results from porosity, radiative/contact-limited grain conduction, and the absence of interstitial gas.

The Bond albedo is low (≈ 0.11), so the surface absorbs most of the incident solar radiation. Topography is extreme by terrestrial standards: multi-kilometer relief is common, and the polar regions in particular contain deep, permanently shadowed craters whose floors never receive direct sunlight. These topographic cold traps are central to the long-term sequestration of volatiles and to the diurnal and seasonal behavior of condensable species such as argon and water.

Surface Temperature Regime

Because of the low thermal inertia and the long lunar day, surface temperature extremes are among the largest of any body in the Solar System:

- At equatorial latitudes the daytime maximum reaches approximately 390–400 K, while the nighttime minimum falls to 90–100 K—a diurnal swing of roughly 300 K.
- Polar sunlit slopes experience lower peak temperatures and strong seasonal variation.
- Permanently shadowed regions routinely remain below 110 K; many locations stay in the 20–50 K range, and some of the coldest measured surfaces in the inner Solar System (historically reported near or below ~25 K) occur in specific polar craters.

These temperatures control residence times, accommodation, adsorption, desorption, and cold trapping. Helium and neon are treated as noncondensable under ordinary lunar conditions: their nightside enhancements arise mainly from ballistic redistribution over a temperature field (approximately the Hodges–Johnson $T^{-5/2}$ behavior), not from a sunrise release of a condensed inventory. They may interact weakly with surface sites without becoming cold-trapped in the sense applicable to ^{40}Ar or H_2O.

Radiation Environment and Solar-Wind Plasma

The Moon has no protective global magnetic field and only a negligible atmosphere, so the surface is directly exposed to the full spectrum of solar electromagnetic radiation and to the solar wind. Solar EUV and UV photons drive photon-stimulated desorption (PSD) of alkali metals and other species. Solar-wind ions (primarily protons and alpha particles traveling at 300–800 km s^{-1}) implant into the regolith, sputter surface atoms, and, after neutralization and recombination, contribute to the neutral hydrogen and helium populations.

Coronal mass ejections can greatly increase incident ion flux and energy. CHACE-2 observations during the 10 May 2024 extreme event showed more than an order-of-magnitude increase in total dayside exospheric number density and pressure; attributing the increase to specific refractory neutrals remains model- and mass-channel-dependent.

Magnetic Field: Absence of a Global Field and Presence of Crustal Anomalies

The Moon lacks a global dynamo field, but localized crustal anomalies—many prominent on the farside—deflect incident plasma and create small plasma cavities or ‘mini-magnetosphere’ structures. Their characteristic horizontal scales range from tens to hundreds of kilometers, while stand-off altitudes are generally much smaller. They locally modify precipitation, sputtering, charging, and sheath structure.

Monthly Passage through Earth’s Magnetotail

For several days around full Moon the Moon traverses Earth’s magnetotail. Direct solar-wind proton and alpha-particle flux is then replaced by magnetospheric lobe or plasma-sheet populations whose density, temperature, composition, and flow depend on the Moon’s position. The best-established exospheric response is a reduction and recovery of solar-wind-derived helium; sodium morphology and effective temperature can also change. A generic statement that all plasma densities simply ‘drop’ is not valid.

This monthly modulation provides a natural experiment that helps separate solar-wind-driven processes from other source mechanisms.

Summary of Atmospheric Implications

The combination of low gravity, extreme temperature swings, direct exposure to solar radiation and plasma, the presence of cold traps, and the monthly magnetotail transit creates an environment in which the atmosphere is continuously generated at the surface, travels on ballistic trajectories, and is lost either by escape, photoionization, or re-adsorption. Every subsequent chapter builds on these boundary conditions.

Part 4 — Nature of the Lunar Atmosphere: Surface-Bounded Exosphere

Definition of an Exosphere and the Surface-Bounded Case

An exosphere is the outermost region of an atmosphere in which the mean free path of particles becomes comparable to or greater than the local scale height. In this regime collisions between particles are rare, and individual atoms or molecules travel on independent trajectories under the influence of gravity (and, when relevant, radiation pressure or electromagnetic forces).

On Earth, a conventional exobase marks the transition from a collisional thermosphere to collisionless motion, typically several hundred kilometers above the surface. The Moon has no underlying collisional atmosphere: its solid surface is the source-and-sink boundary and is often called the exobase by analogy. 'Surface-bounded exosphere' is the more physically precise description.

Near-surface neutral densities are typically only 10^3–10^5 cm^{-3} for the major measured gases. With plausible neutral collision cross sections, mean free paths are much larger than species scale heights and often of lunar-radius scale or greater, so neutral–neutral collisions are negligible for the native quiet exosphere.

Contrast with Collisional Atmospheres

Property	Collisional Atmosphere (Earth)	Surface-Bounded Exosphere (Moon)
Mean free path	≪ scale height	≫ scale height
Particle interactions	Frequent collisions maintain Maxwellian distributions and continuum fluid behavior	Particles move independently; collisions rare
Governing physics	Hydrostatic balance, Navier–Stokes equations, thermodynamics of continuous media	Kinetic theory, ballistic trajectories, surface interaction physics
Vertical structure	Distinct layers (troposphere → thermosphere → exosphere)	Single surface-bounded exosphere
Ability to support weather systems	Yes (pressure gradients, winds, waves, instabilities)	No classical weather systems

On Earth, pressure gradients drive winds, and molecular collisions allow the atmosphere to behave as a fluid. On the Moon there is no continuum fluid; there are only individual particles on ballistic paths. Concepts such as geostrophic balance, baroclinic instability, or Hadley cells have no direct counterpart.

Collisionless Regime and Independent "Atmospheres"

Because collisions are negligible, each chemical species evolves essentially independently. Helium does not "feel" the presence of argon or sodium in any dynamical sense. Each species therefore constitutes its own "atmosphere," with its own source rates, loss rates, scale height, diurnal behavior, and spatial distribution. This independence of species, already emphasized in early reviews (Stern, 1999), remains a defining feature of surface-bounded exospheres.

This independence is both a simplification and a complication. It simplifies modeling (one can treat species separately), but it also means that the total atmospheric density is simply the sum of the individual species densities, each of which can vary dramatically with local time, latitude, and solar activity.

Ballistic Trajectories as the Dominant Motion

Once a particle leaves the surface with a given velocity vector, its subsequent motion is governed almost entirely by lunar gravity (and, for some species, by solar radiation pressure). Under the constant-g approximation the trajectory is a simple parabola:

- Time of flight (round-trip): $t_D = 2\, v_z / g$
- Maximum height: $z_{max} = v_z^2 / (2g)$

Under point-mass inverse-square gravity, trajectories are exact Keplerian ellipses or hyperbolas. Thermal hop lengths range from kilometers to much farther distances depending on species mass, temperature, launch-angle distribution, and surface accommodation; a few to a few tens of kilometers is representative only for some heavier, colder populations. Non-thermal particles released by sputtering or micrometeoroid impacts can reach hundreds or thousands of kilometers in altitude and, in the case of sodium, form the extended lunar sodium tail that stretches anti-sunward for many lunar radii.

Implications for Hydrostatic Balance, Fluid Dynamics, and Familiar Meteorological Concepts

Several foundational ideas from terrestrial meteorology must be modified or abandoned:

- **A barometric-looking density law can emerge statistically for a collisionless ensemble whose surface launch distribution is thermal. It is mathematically equivalent to the hydrostatic result only under restricted equilibrium assumptions; no fluid element or collision-maintained pressure gradient is required.**
- **Scale height remains useful as a local energy-to-gravity ratio, H = kT/(mg). For a collisionless population, however, T characterizes the launch or velocity distribution, and a nonthermal distribution may not possess one unique scale height.**
- **Pressure** can be represented approximately by p = n k T for an isotropic thermal population, yet pressure gradients do not drive winds in the usual way because there is no fluid to respond. Anisotropic or hot populations require a pressure tensor or the full velocity distribution; an effective temperature is only a parameterization.
- **Classical winds are replaced by ballistic lateral transport. Noncondensable gases redistribute statistically toward colder regions, while condensable or strongly adsorbing species can be stored on the nightside and released as surface temperature rises.**
- **Weather** in the classical fluid-dynamical sense does not exist. Temporal variability is dominated by the diurnal cycle of surface temperature, solar illumination, solar-wind flux, and occasional impulsive events (meteoroid streams, CMEs).

In short, the lunar atmosphere is best understood through kinetic theory and surface physics rather than through the fluid-dynamical framework that dominates classical meteorology. The chapters that follow develop the sources, sinks, composition, and dynamics of this collisionless system in detail.

Part 5 — Composition of the Lunar Exosphere

The lunar exosphere is extremely tenuous and chemically diverse. Its instantaneous composition results from surface release, ballistic transport, surface exchange, ionization, and escape. Because neutral–neutral collisions are negligible, each species evolves largely independently and can have a distinct spatial and temporal distribution.

Major Noble-Gas Constituents

The three most abundant species under typical conditions are the noble gases helium, neon, and argon.

Helium (He) is supplied mainly by solar-wind alpha particles that are implanted, neutralized, and later released from the regolith. It is noncondensable under lunar conditions. Its observed maximum near 1–2 a.m. local time is broadly consistent with temperature-controlled ballistic redistribution, while the post-dawn decrease reflects the changing distribution and enhanced gravitational loss. Near-surface densities range from a few $\times 10^3$ to about 6.5×10^4 cm^{-3}.

Neon (Ne) is also largely associated with solar-wind implantation and release. LADEE found a pre-dawn maximum near 4 a.m. local time. Neon is modeled as a surface-accommodated noncondensable gas: the maximum is produced by ballistic redistribution across the diurnal temperature field, not by condensation followed by sunrise desorption. Near-surface densities are generally 10^3–2×10^4 cm^{-3}. Grava et al. (2026) used Diviner temperatures to predict local depletions up to ~18% below ~20 km over warm, rocky terrain such as Tycho and a day–night density crossover near 90–100 km altitude.

Argon is dominated by radiogenic ^{40}Ar produced by ^{40}K decay and released from the interior and regolith. LADEE observed a western-maria enhancement and mission-scale variability of roughly 25%. Cold-surface adsorption and temporary trapping—not necessarily bulk condensation—produce strong local-time and seasonal structure, with a maximum near sunrise and densities reaching roughly 2×10^4–10^5 cm^{-3}. A smaller ^{36}Ar component is associated with the solar wind.

These three species together account for the bulk of the measured neutral density under quiet conditions.

Alkali Metals: Sodium and Potassium

Sodium (Na) and potassium (K) are present at much lower absolute abundances (surface densities typically tens of atoms cm^{-3} for Na), yet they are among the best-observed species because they produce bright resonance-scattering emission lines that can be detected from Earth-based telescopes and from orbit.

Na and K are released by photon-stimulated desorption, ion sputtering, impact vaporization, and thermally modulated exchange with surface reservoirs. Their nonthermal components have characteristic temperatures of several thousand kelvin and apparent scale heights of hundreds to thousands of kilometers. Devaraj et al. (2026), published in The Astrophysical Journal after its April preprint, combined Chandrayaan-2 CLASS, LADEE-UVS, and Diviner data and argued that albedo-driven temperature differences and weakly bound multilayer Na reservoirs strongly control the low-altitude distribution. This is a published interpretation, while the relative source fractions remain an active research question.

Hydrogen Species

Atomic H and molecular H_2 are scientifically important but difficult to inventory. Solar-wind protons implant in the regolith and can be re-emitted as energetic H, recombine to H_2, or participate in OH/H_2O chemistry. LRO/LAMP detected H_2. Impact release, knock-on or chemical sputtering, recombination, diffusion, and geochemical conversion have all been proposed; present observations do not establish one universally dominant H_2 production pathway. Coupled H–H_2–OH–H_2O Monte Carlo models reproduce important features of the observed H_2 distribution while retaining substantial uncertainty in OH and H_2O.

Trace Molecular and Volatile Species

LADEE and earlier Apollo instruments recorded several additional mass channels, but some volatile identifications remain contamination-limited or ambiguous:

- Methane (CH_4): LADEE NMS water- and methane-related channels were affected by getter and hot-filament artifacts, and Apollo LACE methane measurements were contamination-limited.
- Carbon-bearing neutrals: mass 28 is ambiguous among CO, N_2, and Si; neutral CO was not cleanly identified, and CO_2 evidence is limited to tentative mass-channel interpretations and upper limits.
- Indigenous or delivered volatiles remain under investigation, but an ionic detection does not by itself establish a co-located neutral density or an unambiguous neutral parent species.

Secure neutral densities cannot be assigned generically to ambiguous trace mass channels. Terada et al. (2026) measured C^+, N^+, and O^+ with Kaguya and found daily variations in C^+/O^+ and N^+/O^+. They discussed a nitrogen-rich surface reservoir or N-free CO/CO_2 as possible contributors. These are ion measurements and source inferences; they do not by themselves establish neutral CO, N_2, or CO_2 densities.

Refractory Elements

Impact vaporization and ion sputtering can release O, Si, Al, Mg, Fe, Ca, Ti, and other refractory elements. Their quiet-time neutral abundances remain poorly constrained. During the May 2024 extreme CME, Chandrayaan-2/CHACE-2 measured a large increase in total dayside number density and pressure, consistent with enhanced sputtering, but the observation did not uniquely resolve a complete refractory-neutral composition.

Isotopic Composition and Source Constraints

K and Rb isotopes in Apollo soils were modeled as recording at least ~70% impact-vaporization loss relative to at most ~30% solar-wind sputtering over long times. This is a time-integrated constraint on the modeled K–Rb system, not a universal source fraction for all lunar species.

Spatial and Temporal Compositional Variations

Composition is neither uniform nor constant:

Diurnal cycle – The strongest variation. LADEE found helium peaking around 1–2 a.m., neon near 4 a.m., and radiogenic ^{40}Ar near sunrise; Na and K also vary strongly with illumination and surface temperature.

Latitude and topography – Polar cold traps sequester volatiles; crustal magnetic anomalies locally reduce sputtering.

Solar activity – Solar-wind changes and CMEs alter implantation and sputtering. Large changes in total density are observed, but species-resolved refractory/volatile ratios require instrument-specific interpretation.

Magnetotail passage – Direct solar-wind supply is interrupted. Helium shows a documented depletion and recovery; responses of longer-lived or surface-stored species can be delayed and need not track the plasma change immediately.

Because each species responds differently to these drivers, the relative composition of the lunar exosphere changes continuously. The total number density is simply the sum of the individual contributions at any given location and time.

Part 6 — Structure: Density, Pressure, Temperature, and Vertical Profiles

The lunar exosphere has no collision-maintained fluid layers. Each species' distribution reflects its launch-energy distribution, ballistic accessibility, surface interaction, ionization, and escape; these processes range from prompt to geologically slow rather than being uniformly rapid.

Surface Number Densities and Diurnal Dependence

Surface number densities are the fundamental observable and model constraint. They vary by orders of magnitude from species to species and, for most species, by large factors over the course of a lunar day.

Typical quiet-time ranges (near the surface) include:

- Helium: a few $\times 10^3$ to ~6.5×10^4 cm^{-3}, peaking around 1–2 a.m. local time
- Neon: 10^3–2×10^4 cm^{-3}, with a pre-dawn peak near 4 a.m. local time
- ^{40}Ar: 2×10^4–10^5 cm^{-3} at sunrise, declining through the night as atoms adsorb onto the cooling surface
- Sodium: typically tens of atoms cm^{-3} at the surface (column densities ~10^9–10^{10} cm^{-2})
- Trace and refractory species: generally lower, but capable of large transient increases during solar storms

The diurnal cycle is dominant, but the mechanisms differ. Noncondensable He and Ne develop nightside maxima through ballistic redistribution over the surface-temperature field. ^{40}Ar is strongly affected by cold-surface adsorption and release near dawn. Na and K undergo illumination-dependent and thermally modulated surface exchange rather than behaving as simple bulk condensates.

Total Mass and Equivalent Surface Pressure

Legacy global-inventory estimates of roughly 10–25 tonnes imply an equivalent mean load of order 10^{-10}–10^{-9} Pa (traditional benchmark 3×10^{-10} Pa). Both values are model-dependent summaries, not a simultaneously measured global state, and the pressure is not dynamically homogenized as in a collisional atmosphere.

Temperature: Thermal versus Non-Thermal Components

Two distinct thermal regimes coexist.

Thermal components are those that have accommodated to the local surface temperature (roughly 100 K on the nightside to ~390–400 K on the dayside equator). For these populations the scale height is $H = kT/(mg)$. At 100 and 400 K, respectively, the values are about 128 and 513 km for He, 25 and 102 km for Ne, 13 and 51 km for Ar, and 22 and 89 km for Na. Hundreds of kilometers therefore mainly apply to helium or to hot, non-thermal populations, not cold heavy noble gases.

Non-thermal (hot) components arise from energetic release processes—photon-stimulated desorption, ion sputtering, and micrometeoroid impact vaporization. Their velocity distributions can be parameterized by effective temperatures of 1000–9000 K (especially for sodium), but such effective temperatures do not imply thermal equilibrium. The corresponding apparent scale heights are large (often 500–2000 km or more), allowing particles to reach high altitudes and, in the case of sodium, to form the extended lunar tail.

Many species exhibit both a cold (thermal) and a hot (non-thermal) population simultaneously. The relative importance of each component depends on the dominant source mechanism at that location and time.

Scale Heights and Vertical Structure

For a flat, constant-g surface and a Maxwell–Boltzmann-flux launch distribution, the thermal ballistic number density is exactly exponential, $n(z) = n_0 \exp(-z/H)$. In spherical gravity the full-Maxwellian factor is $\exp[GMm(kT)^{-1}(1/r - 1/r_0)]$, but a real exosphere occupies only accessible parts of velocity space; the

Chamberlain partition functions supply that correction. Other launch laws and surface roughness can produce more ground-hugging profiles.

Key practical points:

- Scale heights are species-dependent and process-dependent.
- Heavier species and colder surfaces produce smaller scale heights.
- Hot non-thermal populations dominate the high-altitude structure.
- The classical Chamberlain formalism and modern Monte-Carlo trajectory models are the standard tools for calculating realistic vertical profiles.

Day–Night Contrasts and Terminator Behavior

Near sunrise, strongly adsorbing or condensable species such as ^{40}Ar can be released as residence times collapse. Noncondensable He and Ne do not require a stored condensed reservoir: their local-time curves reflect ballistic transport, source history, and loss. Alkali behavior combines surface reservoirs, illumination, and nonthermal release.

Horizontal transport is therefore not one universal warm-to-cold ‘wind.’ Noncondensable gases statistically concentrate over colder regions in ballistic equilibrium; sticky volatiles migrate through repeated hops and surface residence and may reach cold traps. Grava et al. (2026) predict that neon is denser on the nightside below ~90–100 km but denser on the dayside above that altitude because the warmer dayside population has a larger vertical extent.

Summary

The structure of the lunar atmosphere is therefore best described statistically:

- Near-surface densities set by species-specific source, loss, and surface-exchange balances.
- Vertical profiles set by the energy distribution of particles leaving the surface.
- Horizontal structure dominated by the extreme diurnal temperature cycle and the presence of permanent cold traps.

There is no classical weather, no pressure-driven wind systems, and no layered thermal structure of the terrestrial type. What exists is a set of overlapping, collisionless, ballistic “atmospheres,” each responding in its own way to the thermal, radiative, and plasma environment of the Moon.

Part 7 — Sources of Atmospheric Constituents

The native exosphere is continually renewed, but 'lifetime' must be defined. A ballistic flight may last minutes to hours; a fitted density response may be days; a photoionization lifetime may be months; and a molecule stored in a PSR may remain for geologic time. Source and loss rates must therefore be stated by species and process.

Micrometeoroid Impact Vaporization (MIV)

Micrometeoroid impact vaporization is an important global source of alkalis, moderately volatile elements, and refractory vapor. Its dominance is well supported for some time-integrated isotope systems, especially K–Rb, but should not be assumed for every species or every instantaneous condition. Typical impact speeds are of order 10–20 km s^{-1}, with a broad distribution.

A K–Rb isotope model inferred ≥70% impact-vaporization loss relative to ≤30% ion sputtering in the long-term K–Rb record. Impact vaporization also supplies Na, K, and refractory atoms and is enhanced during meteoroid streams, but species-specific source fractions remain uncertain.

Solar-Wind Ion Sputtering

The solar wind primarily bombards surfaces directly exposed to it. Protons and alpha particles with energies of ~1 keV per nucleon eject surface atoms through momentum transfer (physical sputtering). Plasma access is complicated by the lunar wake, magnetotail passages, and crustal magnetic fields, so sputtering is not strictly confined to a simple geometric dayside. Sputtering yields depend on ion energy, incidence angle, and surface composition.

Sputtering produces energetic ejecta and can become much stronger during CMEs. The May 2024 CHACE-2 event demonstrates an order-of-magnitude change in total dayside density/pressure, not a uniquely resolved inventory of refractory neutrals. Separately, Terada et al. (2026) found daily C^+, N^+, and O^+ variations and argued that daytime solar-wind sputtering of a nitrogen-rich reservoir is one plausible major ion source; N-free CO/CO_2 was an alternative discussed by the authors.

Photon-Stimulated Desorption (PSD)

Ultraviolet and extreme-ultraviolet photons from the Sun can directly eject atoms adsorbed on or near the surface. Photon-stimulated desorption is particularly efficient for the alkali metals (Na and K). Laboratory and observational evidence shows that PSD produces a characteristic non-thermal velocity distribution and is strongly modulated by solar UV flux and by the availability of atoms in the topmost atomic layers of the regolith.

PSD operates only on the illuminated hemisphere and ceases at night, contributing to the pronounced day–night asymmetry of the sodium and potassium exospheres.

Thermal Desorption and Sublimation

Thermal desorption is important for species with finite surface residence, especially ^{40}Ar and water-group molecules. At dawn, rapidly falling residence times can generate a release maximum. Devaraj et al. (2026), now a peer-reviewed ApJ paper, proposed that weakly bound multilayer Na reservoirs and albedo-driven temperature differences dominate the low-altitude Na pattern, with nonthermal processes contributing more strongly aloft. The quantitative partition among mechanisms remains model-dependent.

In the coldest permanently shadowed regions, condensation and long-term retention dominate because water ice and other volatiles can remain stable over geologic time. Sublimation is most important at warmer PSR margins, on transiently illuminated surfaces, and where ice has been disturbed or newly exposed.

Radiogenic Outgassing (^{40}Ar)

A unique and quantitatively important source is the production of ^{40}Ar by radioactive decay of ^{40}K in the lunar crust and mantle. Production is widespread and nearly steady on human timescales, but diffusion, storage, and release through the regolith vary in space and time. LADEE observed an enhancement over the western maria/Oceanus Procellarum region and about 25% temporal variation. Nightside adsorption and release near sunrise make ^{40}Ar a valuable tracer of surface-temperature-controlled processes. Radon-222 and its progeny have likewise been used as tracers of localized outgassing. A 2026 EGU conference abstract reported preliminary DORN results from the single Chang'E 6 farside site, with no detected radon and only trace polonium (Meslin et al., 2026). Those site-specific preliminary measurements should not be treated as a global radon flux or as a general constraint on lunar-regolith permeability.

Solar-Wind Implantation, Neutralization, and Chemical Sputtering

Implanted solar-wind protons and alpha particles are neutralized and can later be released. This pathway is central to lunar He and is an important source for Ne, H, and H_2. For H_2, recombination, diffusion, impact release, and chemical or knock-on sputtering remain competing or coupled pathways rather than a settled single dominant mechanism.

Because these sources are directly tied to the solar-wind flux, they are strongly modulated by solar activity and by the Moon's monthly passage through the Earth's magnetotail (when the solar wind is largely excluded).

Possible Terrestrial Contribution via the Magnetotail

A more recently discussed source is the delivery of atoms and ions from Earth's upper atmosphere. When the Moon is inside the terrestrial magnetotail, particles that have escaped Earth's atmosphere can reach the lunar surface. Evidence for terrestrial nitrogen and other species in lunar soils has been interpreted by some authors as indicating a long-term contribution from this pathway, although the quantitative importance for the present-day exosphere remains an active research topic.

Transient and Anthropogenic Sources

Several episodic sources can temporarily dominate local or even global densities:

- Meteoroid streams — Enhanced impact vaporization during major showers produces measurable increases in sodium and other species.
- Coronal mass ejections — Enhanced ion precipitation can raise total exospheric density and pressure by more than an order of magnitude; species-resolved changes depend on instrument response and source modeling.
- Spacecraft activity — Exhaust from landers and the outgassing of habitats or rovers can locally overwhelm the native exosphere. Even a single lunar lander can temporarily dominate the gas density in its vicinity.

Relative Importance and Species Dependence

No single mechanism supplies all species. A useful working summary is:

Source mechanism	Primary species affected	Temporal character
Micrometeoroid impact vaporization	Na, K, refractories, many volatiles	Steady + stream enhancements
Solar-wind ion sputtering	Refractories, Na, K, O, etc.	Quiet + strong CME spikes
Photon-stimulated desorption	Na, K	Directly illuminated surfaces
Thermal desorption / sublimation	^{40}Ar, H_2O-group, other volatiles	Strongly diurnal / seasonal
Radiogenic outgassing	^{40}Ar	Production steady; release variable
Solar-wind implantation/re-release	He, Ne, H, H_2	Solar-wind modulated

The interplay among these sources, modulated by surface temperature, solar activity, and geometry, produces the complex, time-varying composition and structure described in the preceding chapters.

Part 8 — Loss Processes and Sinks

The exosphere remains tenuous because species-specific losses and surface reservoirs balance species-specific sources. The often-quoted global inventory of order 10–25 tonnes is a legacy estimate; it should not be combined with a single universal lifetime.

Thermal (Jeans) Escape

Thermal escape is the upward flux carried by the high-speed portion of a velocity distribution whose total speed exceeds $v_{es}c = 2.38$ km s^{-1}. Individual particles, not an average 'thermal speed,' satisfy the escape condition.

The efficiency of Jeans escape is governed by the Jeans parameter:

$$\lambda = GMm/(kTr) = v_{es}c^2/{v_{mp}}^2, \text{ with } v_{mp} = \sqrt{(2kT/m)}$$

Because the Jeans flux contains $(1 + \lambda)e^{-}\lambda$, it changes exponentially rather than at a sharp cutoff. Small λ gives strong escape; large λ gives a strongly depleted tail. Whether the loss is important also depends on the source rate and available time.

At 400 K, λ is approximately 0.86 for H, 3.4 for He, 17 for Ne, 20 for Na, and 34 for Ar. Thermal escape is therefore strong for H, important for He, and usually weak for cold heavy species; nonthermal source tails can alter that ranking.

For an isotropic Maxwellian at a conventional exobase, integration over upward velocities with $v > v_{es}c$ gives:

$$\Phi_J = (n\, v_{mp} / 2\sqrt{\pi})(1 + \lambda)e^{-}\lambda$$

Photoionization and Pickup-Ion Loss

Solar ultraviolet and extreme-ultraviolet radiation ionizes neutral atoms and molecules. Once ionized, a particle is no longer bound solely by lunar gravity; it feels the electric and magnetic fields of the solar wind (or of the terrestrial magnetotail when the Moon is inside it). The newly created ion is accelerated and typically carried away from the Moon—a process known as pickup-ion loss.

Sunlit photoionization lifetimes are species-dependent and must be distinguished from fitted exospheric response times. Neon's ordinary solar photoionization lifetime is of order six months, whereas lunar helium observations yield an effective decay of about 4.5 days dominated by gravitational loss. A shorter fitted Ne lifetime signals an additional modeled sink or transport mismatch, not a changed atomic photoionization cross section.

Surface Adsorption, Sticking, and Cold Trapping

Not all particles that return to the surface bounce back into the exosphere. Depending on the species, the surface temperature, and the surface composition, an atom may stick (adsorb) with high probability. On the cold nightside and especially in permanently shadowed regions (PSRs), residence times can become extremely long.

- Temporary adsorption on the nightside produces the diurnal density variations observed for ^{40}Ar and contributes to the transport of volatiles toward the poles.
- Permanent or quasi-permanent cold trapping in PSRs removes water and other volatiles from the active exosphere for geologic timescales. Seasonal cold traps near the poles also sequester argon and other species on timescales of months.

Surface sticking is therefore both a temporary sink (nightside) and, for the most volatile species in the coldest traps, a long-term or permanent sink.

Radiation-Pressure Acceleration

Solar radiation pressure exerts a continuous force on atoms that have strong resonance transitions (most notably sodium and potassium). For sodium the acceleration is significant: over a few hours an atom can gain several hundred meters per second of anti-sunward velocity. This force is responsible for the formation of the extended lunar sodium tail that stretches many lunar radii in the anti-sunward direction. Atoms that would otherwise be gravitationally bound can be pushed onto escape trajectories by radiation pressure, providing an additional loss channel for the alkalis.

Energetic Ejection Beyond Escape Speed

When particles are released by energetic processes—micrometeoroid impact vaporization or ion sputtering—a fraction of the ejected atoms already possess speeds greater than lunar escape velocity. These particles leave the system on their first trajectory and never return to the surface. The fraction that escapes promptly depends on the velocity distribution of the source process. Impact vaporization and sputtering both produce high-energy tails, so prompt escape is non-negligible for these sources.

Overall Mass-Loss Rates and Atmospheric Lifetime

A classic global source/loss scale is of order 10 g s^{-1}, with large species- and model-dependent uncertainty; some event or source estimates are higher. Combining 10–25 tonnes with 10 g s^{-1} gives a bulk inventory/source ratio of about 12–29 days. This arithmetic is not a particle lifetime and should never replace species-specific escape, ionization, or surface-residence times.

Different species have different dominant loss pathways:

Species group	Primary loss channels	Representative process-specific timescale
H, He	Prompt/thermal escape + photoionization/pickup	He exospheric decay ~4.5 days; H varies
Ne	Photoionization/pickup + limited escape	Photoionization ~6 months; fitted effective times may be shorter
^{40}Ar	Surface adsorption + photoionization	Exospheric and surface-storage times differ; local-time dependent
Na, K	Photoionization/pickup + radiation pressure + sticking	Commonly hours to days
Refractory atoms	Photoionization/pickup + prompt energetic escape	Process-dependent; prompt ejecta may escape immediately

The multiplicity of source, loss, and surface-storage processes keeps the lunar exosphere at low density. Its instantaneous state reflects species-specific balances rather than a single short lifetime shared by all constituents.

Part 9 — Surface–Exosphere Interactions

In a surface-bounded exosphere the surface is not merely a passive boundary; it is an active participant in the life cycle of every atom and molecule. Particles are repeatedly launched from the surface, follow ballistic trajectories, and return to interact with the regolith again. The physics of these surface encounters—adsorption, desorption, energy exchange, and diffusion—controls residence times, diurnal variability, and the long-term sequestration of volatiles.

Adsorption and Desorption Kinetics

When a particle strikes the lunar surface it may bounce (scatter) or stick (adsorb). The sticking probability depends on the species, the impact energy, the surface temperature, and the chemical nature of the surface site. For many volatiles the sticking coefficient approaches unity at low temperatures.

Thermal residence follows an Arrhenius law and can vary by orders of magnitude among sites. He and Ne have very short residence times under ordinary lunar conditions and are treated as noncondensable; ^{40}Ar can be temporarily adsorbed on cold terrain, while H_2O can be retained for extremely long intervals in sufficiently cold, stable settings.

A heterogeneous regolith has a distribution of binding energies rather than one value. Grava et al. (2026) predict topography-driven Ne variations despite Ne remaining noncondensable. Devaraj et al. (2026), now peer-reviewed, interprets Na data using weakly bound multilayer reservoirs and temperature-dependent release; this is a published model interpretation, not direct imaging of the reservoir.

Thermal Accommodation and Partial Thermalization

Not every particle that leaves the surface is fully thermalized to the local surface temperature. Accommodation refers to the degree to which an incoming particle exchanges energy with the surface before departing.

- Fully accommodated particles leave a thermal surface with a Maxwell–Boltzmann-flux (Knudsen) distribution: the ordinary Maxwellian is weighted by the outward normal velocity. This distinction matters for hop-height and hop-length statistics.
- Partially accommodated or non-accommodated particles retain memory of their original energy (for example, the high energies imparted by sputtering or impact vaporization).

Laboratory experiments and exospheric observations show that alkali metals released by photon-stimulated desorption or sputtering often leave with effective temperatures of several thousand kelvin—far above the surface temperature. In contrast, radiogenic argon that has diffused through the regolith and thermally desorbed is much closer to local thermal equilibrium. The degree of accommodation therefore depends on both the release mechanism and the species.

Diffusion within the Regolith and Vapor Pumping

The uppermost regolith is porous. Atoms can diffuse into the pore space and later return to the surface. This subsurface reservoir is especially important for argon and for water-group molecules. A 2026 EGU conference abstract reported preliminary, site-specific Chang'E 6/DORN radon and polonium results from one farside location (Meslin et al., 2026). Those results do not yet establish a global noble-gas diffusivity or permeability for the regolith. Geochemical conversion reactions further couple hydrogen-bearing species, allowing implanted solar-wind hydrogen to be redistributed among H, H_2, OH, and H_2O before release (Smolka et al., 2023).

A related process is vapor pumping (or thermal pumping). Because the temperature dependence of residence time is strongly nonlinear, repeated day–night temperature cycles can drive a net downward migration of volatiles into the colder subsurface. Over many cycles this can enrich the near-surface regolith in certain species relative to the immediate surface concentration. The same physics, operating in reverse, can later release those volatiles when temperatures rise.

Role of Surface Composition, Grain Size, and Topography

The lunar regolith is not uniform. Mature soils, immature ejecta, mare basalts, and highland anorthosites present different mineralogies and different densities of adsorption sites. Grain-size distribution affects both the surface area available for adsorption and the thermal inertia of the uppermost layer. Topography introduces shadows, slope-dependent illumination, and local variations in surface temperature that modulate adsorption and desorption rates on scales from centimeters to kilometers.

Cold-Trap Physics and Volatile Sequestration

In the coldest PSRs, exposed water ice has extremely low sublimation rates, and buried or shaded deposits can be stable for geologic intervals. Stability still depends on exact temperature, illumination, burial depth, impact gardening, and sputtering; not every molecule entering a PSR is permanently retained.

Seasonally or intermittently cold terrain can temporarily store ^{40}Ar and other volatiles, but the duration and geographic extent are species- and temperature-dependent. Permanent PSRs are the most effective long-term sinks for water and several other volatiles.

Part 10 — Dynamics and Transport

Because the lunar atmosphere is collisionless, classical fluid dynamics does not apply. Transport is accomplished by the ballistic motion of individual particles under gravity, modified by radiation pressure for certain species and by occasional interactions with the ambient plasma.

Ballistic Hopping and Hop-Length Statistics

A particle that leaves the surface with vertical velocity component v_z follows a ballistic trajectory and returns to the surface after a flight time $t_D = 2 v_z / g$ (under the constant-g approximation). The maximum height reached is $z_{max} = v_z^2 / (2g)$.

Thermal hop lengths depend strongly on species mass, temperature, launch-angle distribution, and surface accommodation. A few kilometers to a few tens of kilometers is representative for some heavier, colder populations, while light or warm species can travel much farther. Non-thermal particles released by sputtering or impacts can hop hundreds of kilometers or more. The hop-length and flight-time distributions determine effective horizontal transport and migration toward the nightside and poles.

Lateral Redistribution and Global Transport

Repeated hops create global redistribution, but the mechanism depends on surface interaction. Noncondensable gases attain higher near-surface density over colder terrain through ballistic statistics. Sticky species can undergo a random walk with long surface residence and a net tendency toward stable cold traps. Dawn release applies mainly to species that were actually stored on the cold surface.

Light noncondensable species usually have larger scale heights and longer hops. ^{40}Ar and water-group species are more strongly controlled by adsorption and residence time; mass alone does not determine transport.

Influence of Topography, Slopes, and Temperature Gradients

Local topography changes solar incidence, shadowing, temperature, and the orientation of the surface normal from which particles are emitted. Shadowed terrain can be a temporary or permanent cold trap. Roughness also changes the outgoing angular distribution and can create a near-surface ground-hugging component, so high-resolution temperature and shape models improve exosphere simulations.

Radiation-Pressure Effects on Trajectories

For sodium and potassium, solar radiation pressure is non-negligible. The continuous anti-sunward acceleration distorts ballistic trajectories into curved paths and ultimately produces the extended lunar sodium tail. Atoms that would remain gravitationally bound in the absence of radiation pressure can be driven onto escape trajectories, linking the dynamics of the alkali exospheres directly to solar photon flux.

Lunar Sodium Tail and Extended Alkali Exosphere

The sodium tail is the escaping, high-energy extension of the Moon's alkali exosphere. Photon-stimulated desorption, solar-wind sputtering, and micrometeoroid impact vaporization release Na and K from the regolith with a range of initial speeds. The faster fraction reaches high altitudes, and resonant solar radiation pressure—especially strong for sodium at the D lines—accelerates atoms anti-sunward. Potassium is governed by related source and radiation-pressure physics, but the much brighter and more extensively mapped distant structure is the sodium tail.

The tail is not a static appendage. Its density and velocity structure integrate surface release over the preceding several days and depend on the source-speed distribution, photoionization loss, the solar resonance-line profile,

and observing geometry. Sodium has been detected at and beyond the Earth–Moon distance, demonstrating that the tail is an atmospheric-escape feature rather than merely a high-altitude bound corona.

Near new Moon, the anti-sunward tail is directed approximately toward Earth. Terrestrial gravity deflects and focuses part of the diffuse sodium population into an enhanced beam that appears from the ground as a faint, roughly three-degree “Sodium Moon Spot” near the antisolar direction. The emission is sodium resonance scattering and is far below naked-eye visibility, but narrowband all-sky imaging and spectroscopy can measure its brightness, morphology, and line-of-sight velocity (Smith et al., 1999; Matta et al., 2009; Baumgardner et al., 2021).

Tail brightness varies from lunation to lunation. Meteoroid impacts can inject hot sodium, including the strong enhancement associated with the 1998 Leonid interval, while solar-wind conditions, photon-stimulated desorption, surface-reservoir availability, lunar distance, and viewing geometry also affect the signal. Consequently, the distant tail is a time-integrated diagnostic of energetic sodium release and escape; it should not be interpreted as a direct map of the instantaneous near-surface sodium density.

Interaction of Neutrals with the Ambient Plasma Flow

Neutral–plasma reactions are species-dependent. Photoionization is usually the clearest route to pickup-ion loss; electron impact and charge exchange can matter in particular plasma regimes, but charge exchange is negligible for some species such as Ne in recent lunar models. Crustal anomalies modify the incident plasma and therefore local source and ionization conditions.

Summary of Dynamical Picture

The dynamics of the lunar exosphere can be summarized as a continuous cycle of ballistic hops, surface interactions, and loss:

- Particles are released from the surface by one of the source mechanisms.
- They follow ballistic (or radiation-pressure-modified) trajectories.
- They return to the surface, where they may stick, thermalize, or bounce.
- Over many cycles, noncondensable populations redistribute according to temperature-dependent ballistic transport, while adsorbing species can migrate toward and remain in colder terrain.
- They are ultimately lost by escape, photoionization/pickup, or permanent cold trapping.

There is no pressure-driven wind field, no turbulence in the fluid sense, and no classical circulation cells. The “circulation” that exists is the statistical outcome of millions of independent ballistic trajectories shaped by gravity, surface temperature, radiation pressure, and plasma interactions.

Part 11 — Temporal Variability

The lunar exosphere is never in a true steady state. Its densities, composition, and spatial structure change continuously on timescales ranging from hours to years. Understanding these temporal variations is essential both for interpreting observations and for predicting the environment that future explorers will encounter.

The Diurnal Cycle

The dominant variability for most species is the diurnal cycle driven by the extreme day–night temperature contrast and the changing illumination.

- Helium and neon have distinct nightside maxima: LADEE found helium peaking around 1–2 a.m. local time and neon near 4 a.m.
- ^{40}Ar is strongly affected by cold-surface adsorption and dawn release. Na and K also vary with local time, but their behavior reflects illumination, thermal reservoir exchange, sputtering, and impacts rather than simple condensation alone.
- Photon-stimulated desorption requires illumination. Solar-wind sputtering primarily affects directly exposed surfaces, but plasma access through the wake, magnetotail conditions, and crustal magnetic fields complicates a strict dayside-only description.

The result is that the relative composition of the exosphere changes systematically around the clock. A measurement made at local noon is not representative of conditions at local midnight or at the terminators. Published peer-reviewed Kaguya measurements of C^+, N^+, and O^+ display pronounced daily variations in their relative ratios (Terada et al., 2026), reinforcing that compositional change with local time is a general feature of the lunar exosphere across both neutral and ionic species.

Lunar-Phase and Magnetotail Effects

For several days around full Moon the Moon passes through the Earth's magnetotail. During this interval the solar wind is largely excluded. The consequences include:

- Interruption of direct solar-wind implantation, with the clearest rapid response observed in helium; longer-lived species may respond more slowly.
- Replacement of solar-wind plasma by magnetotail lobe or plasma-sheet populations; density and temperature may rise or fall depending on the region crossed.
- Alterations in the effective temperature and morphology of the sodium exosphere, which have been observed from the ground and from orbit.

These magnetotail passages provide a natural experiment that helps separate solar-wind-driven processes from other sources.

Seasonal Modulation

Although the lunar axial tilt is only ≈ 1.54°, it is sufficient to produce seasonal effects at high latitudes. Regions near the poles experience long periods of continuous sunlight or continuous shadow depending on the season. Seasonal cold traps form and disappear, sequestering and later releasing argon and other volatiles. The area of surface cold enough to trap water and other species expands and contracts over the course of the year, modulating the polar volatile reservoirs and the high-latitude exosphere.

Response to Solar Activity and Coronal Mass Ejections

CMEs can sharply enhance ion precipitation and sputtering. During the 10 May 2024 extreme event, CHACE-2 measured more than an order-of-magnitude increase in total dayside exospheric number density and pressure. This is strong evidence of a global exospheric response, but not a complete species-by-species refractory inventory.

Meteoroid-Stream Enhancements

When the Moon encounters a major meteoroid stream, the impact vaporization rate rises. Ground-based observations have recorded clear increases in sodium emission during several streams. These events are short-lived (hours to a day or two) but demonstrate that the impact-vaporization source is not perfectly steady.

Longer-Term Evolutionary Changes

Over geologic time the lunar exosphere has evolved as the impact flux declined, the solar wind changed, and the inventory of radiogenic argon was slowly depleted. Isotopic studies of returned soils provide a record of time-integrated source contributions. On human timescales, repeated landings, habitat outgassing, and surface operations will introduce localized and potentially global perturbations. Boccelli et al. (2026), published in The Planetary Science Journal 7:113, modeled one prototype module, two vent configurations, and assumed outgassing rates. Its 30–100 m and ≥3 km examples are preliminary, species-, geometry-, and rate-dependent scenario results—not general exclusion radii.

Ancient Lunar Atmosphere

The modern surface-bounded exosphere need not represent every stage of lunar history. During the principal era of mare volcanism, especially before about 3 billion years ago, basaltic eruptions released indigenous volatiles faster than the present-day background sources do. The gases probably included carbon-bearing species, sulfur-bearing species, and water-related volatiles, although the bulk composition, oxidation state, and eruption-by-eruption release rates remain uncertain.

Needham and Kring (2017) combined reconstructed mare-basalt volumes with volatile abundances and estimated that peak outgassing near 3.5 billion years ago could have produced a maximum surface pressure of order 1 kPa. Their time-averaged calculation suggested that the resulting atmosphere might require roughly 70 million years to dissipate. These values are model estimates rather than direct measurements, and they depend on how volcanic volume is distributed among individual eruptions and on the assumed escape physics.

Later eruption-by-eruption analyses argued that most volcanic events were probably too widely separated to maintain one continuously dense atmosphere, so appreciable atmospheres may instead have formed episodically after unusually large or closely spaced eruptions (Head et al., 2020). Escape calculations also span a wide range: a cooler, CO-dominated millibar atmosphere might survive of order 1 million years, whereas strong upper-atmosphere heating and thermal escape could reduce the minimum lifetime to hundreds of years (Tucker et al., 2021). The duration therefore cannot be represented by one universal value.

At millibar-level pressure the ancient atmosphere would have been physically different from today’s collisionless exosphere. Collisions, pressure gradients, winds, an exobase, and global volatile transport would become relevant. Some volcanic water and other condensable material could have migrated to cold polar terrain and contributed to permanently shadowed deposits, but the retained fraction is uncertain. The ancient lunar atmosphere is therefore a plausible, model-supported phase of lunar evolution, not a directly observed or uniquely reconstructed atmospheric state.

Part 12 — Plasma Environment and Lunar Ionosphere

The Moon is not surrounded only by neutral gas. A complex, low-density plasma environment coexists with and interacts with the neutral exosphere. This plasma is generated by photoionization of neutrals, by the solar wind itself, and by electron emission from the surface. Understanding the plasma is essential for a complete picture of the near-lunar environment and for the interpretation of many remote-sensing and in-situ measurements.

Surface Charging, Photoelectrons, and Secondary Electrons

The surface potential is set by current balance and varies with illumination and plasma regime. Sunlit terrain is commonly a few volts positive because of photoelectron emission. Ordinary nightside potentials are negative and can reach tens to hundreds of volts; kilovolt-scale values are associated with energetic-electron or solar-particle events and should not be presented as routine nighttime conditions.

These surface charges create thin plasma sheaths (Debye sheaths) immediately above the surface. The sheath electric fields influence the trajectories of low-energy charged particles and can affect the emission and return of photoelectrons and secondary electrons.

The Tenuous Lunar Ionosphere

The Moon does not possess a dense, global, terrestrial-style ionosphere. ARTEMIS observations in the geomagnetic tail found a recurrent tenuous component averaging ~0.1–0.3 cm^{-3}, while later low-altitude ARTEMIS analyses found no evidence for a steady global population above 35 cm^{-3} at 10–50 km. Some radio-occultation inversions report larger values, but spacecraft charging, geometry, and retrieval assumptions remain debated.

Ions such as He^+, Ne^+, Ar^+, Na^+, and refractory or volatile ions have been detected or inferred in different regimes. An ion measurement constrains the combination of neutral source, ionization, transport, and instrument response; it does not automatically provide the local neutral composition. Theoretical solitary-wave models are hypotheses, not observational determinations of lunar electron density.

Solar-Wind Interaction, Lunar Wake, and Mini-Magnetospheres

The Moon is an obstacle to the solar-wind flow. On the dayside the solar wind strikes the surface directly (except where crustal magnetic fields are strong). Downstream a plasma wake forms: a region of depleted density that gradually refills with distance. The wake is a rich laboratory for plasma physics, containing beams, instabilities, and counter-streaming populations.

Crustal magnetic anomalies produce plasma deflection and small cavities with horizontal scales from tens to hundreds of kilometers; the effective stand-off altitude is much smaller than the horizontal footprint. The term ‘mini-magnetosphere’ is useful but should not imply a scaled copy of Earth’s dipolar magnetosphere.

Pickup Ions

A newly formed ion begins gyromotion and is accelerated by the local convection electric field. Its detected flux depends on the neutral distribution, ionization rate, electromagnetic fields, trajectory history, and instrument acceptance; it is not simply proportional to one local neutral density.

Plasma–Neutral and Plasma–Dust Coupling

Neutral gas, plasma, surface charging, and dust are coupled through ionization, charging currents, impacts, and possibly local dust motion. The strength of each coupling varies by altitude and plasma regime; a dense, collectively behaving dusty plasma has not been established as a persistent global lunar layer.

Summary

The lunar plasma environment is tenuous, highly kinetic, and strongly influenced by the absence of a global magnetic field and by the presence of crustal anomalies. It both arises from and acts back upon the neutral exosphere through ionization, pickup, and surface charging. For future exploration, surface charging and the variable plasma environment also have practical implications for dust adhesion, spacecraft charging, and instrument design.

Part 13 — Dust–Exosphere Coupling

The lunar environment is not a pure neutral-gas + plasma system. LADEE's Lunar Dust Experiment securely detected a permanent, asymmetric impact-ejecta cloud, produced mainly by high-speed cometary micrometeoroids and enhanced during meteor streams. Electrostatic dust mobilization and a dense, high-altitude levitated component are separate questions with different evidence.

Impact-Ejecta Cloud and Proposed Electrostatic Lofting

Modern observations distinguish an established impact-ejecta cloud from more tentative electrostatic-lofting interpretations:

- LADEE/LDEX measured a permanent, asymmetric cloud of impact-generated ejecta, dominated by high-speed cometary micrometeoroids and enhanced during meteor streams.
- Surveyor near-surface horizon glow, Apollo orbital horizon or coronal observations, and Apollo 17 LEAM signals are distinct data sets and do not constitute one uniform detection of a dense levitated layer.
- LADEE found impact-ejected dust but no optically visible levitated-dust effect sufficient to explain the human-visible Apollo horizon glow, placing strong constraints on a dense high-altitude terminator cloud.

Laboratory and charging studies make local, intermittent electrostatic mobilization plausible, but the dense high-altitude terminator population once invoked for Apollo horizon glow remains unconfirmed.

Electrostatic Lofting and Other Mechanisms

The most widely discussed lofting mechanism is electrostatic. On the dayside the surface typically charges positive because of photoelectron emission; on the nightside it charges negative because of the collection of plasma electrons. Near the terminators the surface potential can change rapidly over short distances, producing strong horizontal and vertical electric fields in the plasma sheath.

If a dust grain acquires sufficient charge, the electrostatic force can overcome gravity and cohesion, lifting the grain. Laboratory experiments under vacuum and with UV illumination have demonstrated electrostatic lofting of lunar-simulant grains. Other possible mechanisms include:

- Micrometeoroid impact ejecta (which can throw dust to high altitudes),
- Secondary charging and mobilization by energetic particles,
- Mechanical disturbance by thermal expansion/contraction or by spacecraft activity.

Contribution to Optical Phenomena

A sufficiently dense lofted-dust population could scatter sunlight near the terminators, but LADEE found no optically visible levitated-dust effect capable of explaining the human-visible Apollo horizon glow. The secure modern result is the much more tenuous impact-ejecta cloud. Local electrostatic mobilization remains plausible, whereas a persistent dense high-altitude terminator cloud is unconfirmed and strongly constrained.

Implications for a Multiphase Near-Surface Environment

Charged grains can perturb a sheath when their abundance is high enough, but the ambient impact-ejecta cloud is very tenuous. It is therefore safer to describe the near-surface environment as a coupled surface–plasma–dust system; collective 'dusty plasma' behavior is a possible local regime, not an established global state.

Even if the lofted-dust density is usually low, the coupling remains important for several reasons:

- Dust surfaces can in principle adsorb volatiles, but the importance of moving dust as a volatile reservoir in the natural lunar environment is not yet quantified.
- Charged dust can be transported by electric fields, providing an additional horizontal transport channel.
- Future surface operations will inevitably stir dust, altering the local plasma and neutral environment.

A complete description of the lunar "atmosphere" must therefore acknowledge that neutrals, plasma, and dust form an interconnected system, especially within the first few meters above the surface and near the terminators.

Part 14 — Observational Techniques and Key Datasets

Our knowledge of the lunar exosphere rests on a combination of in-situ measurements, remote sensing, laboratory experiments, and numerical modeling. Each technique has distinct strengths and limitations; together they provide a multi-wavelength, multi-species picture.

In-Situ Mass Spectrometry

Apollo 17 LACE provided the first definitive in-situ neutral-composition measurements and classic He/^{40}Ar local-time curves. Earlier Apollo gauges and ion experiments were scientifically important but more vulnerable to contamination, backgrounds, and non-unique mass assignments.

- Lunar Atmospheric Composition Experiment (LACE) on Apollo 17 provided the classic diurnal density curves for helium and argon.
- SIDE and related Apollo instruments constrained ions, charged-particle events, and the near-surface environment; their mass-to-charge channels should not be treated as unambiguous neutral-species identifications.

Decades later, LADEE's Neutral Mass Spectrometer (NMS) provided systematic in-situ measurements of He, Ne, and Ar, together with searches and constraints for other mass channels, across multiple lunations (2013–2014). LADEE's Ultraviolet–Visible Spectrometer remotely measured Na and K. Together these instruments remain benchmarks for modern exospheric composition and variability studies.

Remote Sensing of Alkali Metals

Sodium and potassium possess strong resonance-scattering lines that can be observed from Earth and from lunar orbit. Ground-based telescopes have mapped the sodium exosphere and its extended anti-sunward tail since the late 1980s. Orbital spectrometers (including LADEE's Ultraviolet–Visible Spectrometer and instruments on other missions) have provided complementary global and temporal coverage. These observations are especially valuable for tracking the hot, high-altitude component and for studying radiation-pressure effects.

UV and Lyman-α Observations

The Lyman-Alpha Mapping Project (LAMP) on the Lunar Reconnaissance Orbiter has measured far-ultraviolet emissions and reflected light, constraining the distributions of H_2 and other species and providing insight into polar volatiles and surface composition. Other UV instruments have contributed additional upper limits and detections of minor species.

Radio Occultation and Ionospheric Measurements

Radio occultations have yielded electron-density profiles, some substantially above in-situ constraints, but retrieval systematics and spacecraft/plasma effects remain debated. ARTEMIS provides direct low-density measurements and upper limits in selected regimes. Separately, a 2026 EGU abstract reported preliminary DORN radon/polonium results from one Chang'E 6 farside site; those site-specific data do not define a global radon flux.

Laboratory Experiments

Controlled laboratory work under vacuum is essential for quantifying the microphysical processes that cannot be measured directly on the Moon:

- Sputtering yields as functions of ion energy, species, and incidence angle,
- Photon-stimulated desorption cross-sections and velocity distributions,
- Adsorption and desorption kinetics on lunar-simulant and analog materials,

- Electrostatic lofting of dust grains under UV and plasma exposure.

These experiments supply the rate coefficients and energy distributions that numerical models require.

Numerical Models and Monte-Carlo Trajectory Simulations

Because the atmosphere is collisionless, the standard modeling approach is the Monte-Carlo test-particle method. Individual particles are launched from the surface with prescribed velocity distributions, followed on ballistic (or radiation-pressure-modified) trajectories, and tracked until they escape, are ionized, or stick. Modern models incorporate:

- Realistic topography and surface-temperature maps,
- Multiple source mechanisms with their characteristic energy distributions,
- Time-variable solar-wind and EUV conditions,
- Surface adsorption/desorption physics,
- Photoionization and pickup-ion loss.

These simulations are the primary tool for converting local measurements into global source rates and for predicting the environment under future exploration scenarios.

Summary of the Observational Landscape

No single technique captures the entire lunar exosphere. In-situ mass spectrometry provides definitive local composition and density; remote sensing of the alkalis supplies global morphology and high-altitude structure; UV observations constrain hydrogen-bearing species and polar processes; plasma instruments and radio occultation characterize the charged environment; laboratory work quantifies the microphysics; and Monte-Carlo models integrate everything into a coherent physical picture. Progress continues to depend on the synergistic use of all these approaches.

Part 15 — Comparative Planetology: The Lunar Exosphere in Context

The Moon is the nearest well-characterized surface-bounded exosphere, but related collisionless atmospheres occur across the Solar System. Comparisons must preserve differences in surface composition, gravity, heliocentric distance, plasma environment, and whether a body has a substantial neutral atmosphere rather than assuming every case is a scaled Moon.

Mercury

Mercury hosts a classic surface-bounded exosphere that shares many traits with the Moon's. Sodium and potassium are prominent and form extended tails shaped by radiation pressure. Calcium, magnesium, and other refractories are also observed. The primary sources—micrometeoroid impact vaporization, photon-stimulated desorption, and solar-wind sputtering—are the same as those operating on the Moon. Differences arise mainly from Mercury's higher surface temperature extremes, stronger radiation-pressure effects (closer to the Sun), and the presence of a weak global magnetic field that partially shields the surface and channels plasma precipitation into cusp regions. The Mercury exosphere is therefore a hotter, more radiation-pressure-dominated counterpart to the lunar system.

Other Airless Bodies

Asteroids can support transient, extremely tenuous clouds produced by impacts, sublimation, or sputtering. Low gravity makes retention inefficient, and direct detections of global steady exospheres remain sparse; 'exosphere' is often an operational label for an intermittent collisionless population.

Europa, Ganymede, and Callisto are not compositionally interchangeable. Europa and Ganymede possess O_2-dominated sputter/radiolysis atmospheres with additional H, O, OH, and H_2O-related components; Callisto has reported CO_2, O_2, and H_2 constraints. Their magnetospheric plasma environment, surface ice, and in some cases intrinsic magnetic field produce dynamics unlike the solar-wind-driven Moon.

Other icy satellites and Kuiper-belt objects. Similar processes operate, scaled by temperature, composition, and plasma environment.

Universal Processes and Local Controls

Across these bodies the same microphysical processes recur:

- Impact vaporization by interplanetary dust,
- Sputtering by solar-wind or magnetospheric ions,
- Photon-stimulated desorption,
- Thermal desorption and cold trapping,
- Photoionization and pickup-ion loss.

What changes from body to body is the relative weighting of these processes, the surface composition that supplies the atoms, the gravity that sets the escape threshold, and the presence or absence of a magnetic field or dense plasma environment. The lunar exosphere therefore serves as a well-calibrated reference case against which more distant or more extreme systems can be interpreted.

Lessons for Broader Planetary Science

Studying the Moon has provided quantitative rates and velocity distributions that are now used in models of Mercury, the Galilean satellites, and even exoplanet surface-bounded atmospheres. Conversely, observations of other bodies (especially the high-quality sodium and calcium data from Mercury) have sharpened questions about the relative importance of impact vaporization versus sputtering that are still being applied back to the Moon. Comparative planetology is therefore a two-way street: the Moon calibrates the rest of the Solar System, and the rest of the Solar System tests the generality of the lunar paradigm.

Part 16 — Applications to Human Exploration and Future Science

As humanity returns to the Moon with sustained presence in mind, the native exosphere ceases to be merely a scientific curiosity and becomes both a resource-relevant environment and a system that will be perturbed by human activity.

Contamination of the Native Exosphere

The global native inventory is only of order tens of tonnes, but descent exhaust does not all remain in the exosphere: much escapes promptly, some adsorbs, and some follows plume–surface trajectories. Nevertheless, even a modest lander overwhelms the native local column, and large vehicles can inject a non-negligible fraction of the estimated global inventory. Boccelli et al. (2026) modeled one habitat/vent scenario; its 30–100 m and ≥3 km examples are species-, geometry-, and rate-dependent, not universal exclusion radii.

Understanding the baseline exosphere is therefore a prerequisite for any scientific investigation that relies on measuring indigenous volatiles. It is also necessary for assessing how human activity will alter the environment that subsequent missions will encounter.

Implications for Polar Resource Prospecting

Permanently shadowed regions are high-priority targets for water-ice and other volatile resources. The same cold-trapping physics that sequesters indigenous water will also trap water and other propellants released by landers and habitats. Distinguishing native polar ice from anthropogenic contamination will require careful pre-landing characterization of the exosphere and of the transport pathways that deliver molecules into the cold traps.

In addition, the diurnal and seasonal migration of argon and other species provides a natural tracer of the temperature-controlled transport processes that also move water. Monitoring these tracers can help map the efficiency of volatile delivery to the poles.

Requirements for Future Instrumentation and Monitoring

A sustained lunar presence will need continuous or frequent monitoring of the neutral and plasma environment. Key requirements include:

- Sensitive mass spectrometers capable of distinguishing native from anthropogenic species,
- Optical or UV remote sensing of the alkalis and other tracers,
- Plasma and electric-field measurements to characterize surface charging and dust mobilization,
- Networks of simple pressure or density sensors to track the evolution of the background atmosphere.

Such monitoring serves both scientific and operational purposes: it protects the integrity of future experiments and provides real-time awareness of the dust and plasma environment that affects surface systems.

The Lunar Atmosphere as a Testbed

Because the lunar atmosphere is so tenuous and responsive, it is an ideal testbed for planetary-protection practices and for environmental-impact monitoring. Lessons learned about how quickly human activity alters a surface-bounded exosphere will be directly applicable to other airless bodies that future missions may visit. In this sense the Moon is not only a destination but also a proving ground for the responsible exploration of the Solar System's many collisionless atmospheres.

Summary

Human exploration will change the lunar exosphere. Baseline measurements, source attribution, and contamination monitoring are essential. A spent Falcon 9 upper stage struck near Einstein Crater on 5 August 2026 in an unintended impact. Same-day spectroscopy detected Na and Li emission consistent with a plume; orbital crater confirmation remained pending at the time of writing. The event is therefore identified as an observed impact, but the preliminary plume signal is not treated as a calibrated exosphere experiment.

Part 17 — Open Questions and Frontiers

Despite the major advances of the Apollo, ground-based, and LADEE eras, the lunar exosphere remains incompletely understood. Several fundamental questions are still open and define the research frontier.

Relative Importance of Source Mechanisms

K–Rb isotope evidence indicates a dominant long-term impact-vaporization contribution for that specific system. The broader instantaneous balance among impacts, sputtering, PSD, thermal release, and implantation remains species-dependent and should not be generalized from K–Rb alone.

The True Role and Density of Lofted Dust

LADEE/LDEX securely established a permanent, asymmetric impact-ejecta cloud. By contrast, whether a persistent or regularly recurring population of electrostatically lofted dust exists at the densities inferred from classic Apollo horizon-glow interpretations remains unresolved and strongly constrained. New in-situ dust and electric-field measurements are needed.

Polar Volatile Inventories and Transport Efficiency

How efficiently are water and other volatiles delivered to permanently shadowed regions? What fraction of the molecules that leave the mid- and low-latitude surface ultimately reach the cold traps versus being lost to space? The answers directly affect estimates of polar resource potential and the interpretation of orbital neutron and UV data.

Anthropogenic Perturbation Timescales and Spatial Scales

As landings and surface operations increase, how rapidly and how far will exhaust gases and habitat leakage alter the background exosphere? Which native species will be most easily masked, and on what timescales will the system recover after a major landing event? Quantitative predictions still carry large uncertainties.

Nightside and Polar Plasma Environment

Most plasma and energetic-particle measurements have emphasized the dayside and the wake. The nightside surface charging environment, especially during energetic-electron events, and the plasma conditions inside polar craters remain sparsely sampled. These regions are precisely where future habitats and resource operations are likely to be located.

Coupled Neutral–Plasma–Dust Models

Existing models treat the neutral exosphere, the plasma, and the dust largely separately. Fully coupled, self-consistent simulations that include charging, lofting, adsorption on dust, and feedback on the sheath electric field are still in their infancy. Developing such models is a clear computational frontier.

Long-Term Evolution and Secular Change

How has the lunar exosphere evolved over geologic time as the impact flux declined and the solar wind changed? Can the present-day isotopic record be inverted to recover the history of source strengths with useful precision? These questions link lunar atmospheric science to the broader chronology of the inner Solar System.

Measurement Gaps

Key observational gaps include:

- Continuous, multi-species, high-cadence density measurements from the surface at a range of latitudes,
- Direct measurement of the velocity distributions of refractories and of water-group species,
- Comprehensive mapping of surface potential and lofted dust across the terminator and into PSRs,
- Simultaneous neutral and ion measurements that can close the source–loss budget for major species.

Addressing these questions will require a combination of new landed instrumentation, orbital remote sensing, laboratory work, and improved numerical models. The coming decade of sustained lunar exploration offers the first real opportunity to close many of these gaps.

Part 18 — Suggested Further Reading and Key Resources

The literature on the lunar atmosphere is extensive. The following selection emphasizes foundational papers, comprehensive reviews, and major mission results that together provide a solid entry point and a path into the research literature. (All are readily available through standard academic channels.)

Foundational and Review Papers

Stern, S. A. (1999). The lunar atmosphere: History, status, current problems, and context. Reviews of Geophysics, 37(4), 453–491.

Classic comprehensive review that still provides excellent physical insight.

Benna, M., et al. (2015). Variability of helium, neon, and argon in the lunar exosphere as observed by the LADEE NMS. Geophysical Research Letters, 42.

Key LADEE noble-gas results.

Colaprete, A., et al. (2016). How surface composition and meteoroid impacts mediate sodium and potassium in the lunar exosphere. Science, 351.

Important constraints on alkali sources from LADEE.

Elphic, R. C., et al. (2014). The Lunar Atmosphere and Dust Environment Explorer mission overview. Space Science Reviews.

Mission context for the modern dataset.

Hodges, R. R. (1973–2016 series of papers). Multiple foundational papers on argon, helium, and the physics of surface-bounded exospheres.

Killen, R. M., & Ip, W.-H. (1999) and subsequent reviews on Mercury and comparative exospheres.

Essential for placing the Moon in context.

Mission Data and Instrument Papers

- Hoffman, J. H., et al. Apollo 17 LACE results (1973 and later analyses).
- LADEE special issues and data archives (NASA Planetary Data System).
- LRO/LAMP papers on H_2 and far-UV observations.
- ARTEMIS, Kaguya, and Chandrayaan plasma and energetic-neutral-atom results.

Laboratory and Theoretical Foundations

Papers on sputtering yields, photon-stimulated desorption cross-sections, and adsorption energies on lunar regolith analogs (various authors in Icarus, JGR Planets, and Planetary and Space Science).

Monte-Carlo modeling methodology papers (e.g., works building on the Chamberlain formalism and modern implementations by Crider, Vondrak, Sarantos, and others).

Broader Context and Exploration Relevance

- National Academies and NASA reports on lunar science and exploration priorities (especially those addressing polar volatiles and the lunar environment).
- Recent reviews on lunar dust and electrostatic lofting.
- Comparative studies of Mercury's exosphere from MESSENGER and BepiColombo.

Data Archives and Ongoing Resources

- NASA Planetary Data System (PDS) – LADEE, LRO, ARTEMIS, and Apollo datasets.
- Ground-based sodium monitoring programs and archives.
- Lunar Reconnaissance Orbiter and commercial lunar payload data as they become available.

This list is intentionally selective rather than exhaustive. A reader who works through the major reviews and the LADEE-era papers will be well positioned to follow the current literature and to identify the open questions outlined in the preceding chapter.

Some Key Literature

- Chamberlain, J. W. (1963). Planetary coronae and atmospheric evaporation. Planetary and Space Science, 11, 901–960.
- Hodges, R. R., Jr., & Johnson, F. S. (1968). Lateral transport in planetary exospheres. Journal of Geophysical Research, 73, 7307–7317.
- Hayne, P. O., et al. (2017). Global regolith thermophysical properties of the Moon from the Diviner Lunar Radiometer Experiment. Journal of Geophysical Research: Planets, 122.
- Schörghofer, N. (2022). Statistical thermodynamics of surface-bounded exospheres. Earth, Moon, and Planets, 126, article 5.
- Halekas, J. S., et al. (2018). A tenuous lunar ionosphere in the geomagnetic tail. Geophysical Research Letters.
- Shen, H. W., et al. (2023). Limits on the density of the lunar ionosphere: ARTEMIS observations. The Astrophysical Journal.
- Smolka, A., et al. (2023). Coupled H, H_2, OH, and H_2O lunar exosphere simulation framework and impacts of conversion reactions. Icarus.
- Dhanya, M. B., et al. (2025). Impact of a coronal mass ejection on the lunar exosphere as observed by Chandrayaan-2. Geophysical Research Letters.
- Grava, C., et al. (2026). Effects of realistic surface temperature variations on the lunar neon exosphere. Planetary and Space Science, 276, 106283.
- Terada, K., et al. (2026). Daily variations of carbon, nitrogen and oxygen ions in a thin lunar atmosphere. Nature Geoscience, 19, 419–424.
- Devaraj, A., et al. (2026). Correlation between lunar surface and exospheric sodium: Effects of albedo-driven temperature on multilayer sodium reservoirs rather than surface-abundance variations. The Astrophysical Journal, 1004, 2.
- Boccelli, S., et al. (2026). Venting and outgassing simulations of pressurized lunar modules: Contamination of the lunar environment. The Planetary Science Journal, 7, 113.

Appendix A — Equation Derivations and Modeling Foundations

This appendix derives the equations used in the text and states the assumptions that make each equation valid. The central distinction is between a collisional gas, whose Maxwellian distribution is maintained locally by collisions, and a surface-bounded exosphere, whose velocity distribution is created at the surface and then transported collisionlessly.

A1. Notation and Regime Diagnostics

Let $\mu = GM$ be the lunar gravitational parameter, r the distance from the lunar center, r_0 the surface or reference radius, $z = r - r_0$ local altitude, m particle mass, T a kinetic or source temperature, k Boltzmann's constant, and $g(r) = \mu/r^2$. A distribution function $f(r, v, t)$ is defined so that $n(r,t) = \int f \, d^3v$.

$$\ell_\mathrm{mfp} = 1/(\sqrt{2}\, n\sigma) \quad (A1)$$

For an ideal hard-sphere gas, ℓ_mfp is the neutral mean free path and σ is an effective collision cross section. The numerical coefficient changes for unequal species and energy-dependent cross sections.

$$\mathrm{Kn} = \ell_\mathrm{mfp}/L \quad (A2)$$

Kn is the Knudsen number for a chosen macroscopic scale L. $\mathrm{Kn} \ll 1$ supports continuum fluid equations; $\mathrm{Kn} \gg 1$ requires kinetic or ballistic treatment. In the native lunar exosphere, Kn is normally very large for any scale height-sized L.

A2. Thermal Distribution at a Surface

Ordinary Maxwellian in a volume

$$f_M(v) = n\,(m/2\pi kT)\text{^}(3/2)\exp[-mv^2/(2kT)] \quad (A3)$$

This isotropic distribution gives the number of particles present per unit velocity-space volume. Its most-probable speed is $v_{mp} = \sqrt{(2kT/m)}$.

Maxwell–Boltzmann-flux distribution leaving a surface

Particles crossing an outward-facing surface are sampled in proportion to their outward normal speed v_z. Therefore the launch distribution is not the ordinary Maxwellian; it is flux weighted. With θ measured from the outward normal:

$$p(v,\Omega)\, dv\, d\Omega = [2a^2v^3e\text{^}(-av^2)\, dv]\,[\cos\theta/\pi\, d\Omega],\ a = m/(2kT) \quad (A4)$$

The speed factor and angular factor each integrate to unity over $v \geq 0$ and the outward hemisphere. The angular law $p(\Omega) = \cos\theta/\pi$ is the Knudsen cosine law. Using the wrong, unweighted Maxwellian changes mean hop times, ranges, and vertical profiles.

A3. Scale Height and the Barometric Factor

Continuum derivation

For a static, isothermal ideal gas in a point-mass gravitational field, hydrostatic balance and $p = nkT$ give:

$$dp/dr = -\rho\,\mu/r^2,\ \ p = nkT,\ \ \rho = mn \quad (A5)$$

$$d\ln n/dr = -m\mu/(kTr^2) \quad (A6)$$

Integrating from r_0 to r:

$$n(r) = n(r_0)\exp\{(\mu m/kT)[1/r - 1/r_0]\} = n(r_0)e\text{^}[\lambda(r)-\lambda_0] \quad (A7)$$

For $z \ll r_0$, g is approximately constant and $1/r - 1/r_0 \approx -z/r_0^2$. Therefore:

$$n(z) = n_0 e^{\wedge}(-z/H), \quad H = kT/(mg) \quad (A8)$$

Why the same factor can appear without a fluid

A collisionless ensemble launched with the Maxwell–Boltzmann-flux law has the same exponential number-density profile in a flat constant-g geometry. The equality is statistical: particles with greater vertical energy spend time at greater height. It does not mean collisions maintain local hydrostatic balance. In spherical geometry, the full-Maxwellian factor in equation A7 must still be multiplied by a velocity-space accessibility factor, derived in the Chamberlain section below.

A4. Ballistic Trajectories

Constant-g approximation

Take z = 0 at a locally flat surface and launch with vertical component v_z0 and horizontal velocity vector v_h. Newton's equation is d²z/dt² = −g. Integrating twice gives:

$$v_z(t) = v_z0 - gt \quad (A9)$$

$$z(t) = v_z0t - \tfrac{1}{2}gt^2 \quad (A10)$$

The returning solution z = 0 other than t = 0 is the hop duration:

$$t_D = 2v_z0/g \quad (A11)$$

At the apex v_z = 0, so:

$$z_max = v_z0^2/(2g) \quad (A12)$$

Horizontal velocity is constant in this approximation. The horizontal displacement vector is:

$$\vec{L} = \vec{v}_h \, t_D = 2\vec{v}_hv_z0/g \quad (A13)$$

Eliminating time gives $v_z^2(z) = v_z0^2 - 2gz$. These equations fail for hops whose altitude or range is a substantial fraction of the lunar radius.

Exact point-mass classification

$$\mathcal{E} = v^2/2 - \mu/r, \quad \vec{h} = \vec{r} \times \vec{v} \quad (A14)$$

Specific orbital energy $\mathcal{E}$ and specific angular momentum h are conserved in a spherical gravitational field. $\mathcal{E} < 0$ gives an ellipse, $\mathcal{E} = 0$ a parabola, and $\mathcal{E} > 0$ a hyperbola. A bound trajectory launched from the solid surface normally intersects the surface again; a bound satellite orbit whose periapsis lies above the surface cannot be populated by simple surface launch alone.

A5. Escape Speed and the Jeans Parameter

Set the specific orbital energy at launch equal to zero to obtain escape speed:

$$0 = v_{es}c^2/2 - \mu/r \Rightarrow v_{es}c = \sqrt{(2\mu/r)} \quad (A15)$$

Compare the gravitational binding energy per particle, μm/r, with thermal energy kT:

$$\lambda(r) = \mu m/(kTr) = v_{es}c^2/v_{mp}{}^2 \quad (A16)$$

The final equality follows because $v_{mp}^2 = 2kT/m$. λ is dimensionless. It is not a switch: the escaping Maxwellian tail decreases continuously as approximately $e^{-\lambda}$.

Illustrative lunar surface Jeans parameters

Species	λ at 100 K	λ at 400 K
H	3.42	0.86
H_2	6.84	1.71
He	13.59	3.40
Ne	68.49	17.12

Species	λ at 100 K	λ at 400 K
Na	78.03	19.51
Ar	135.59	33.90

These values use the mean lunar radius and are illustrative. A nonthermal source distribution cannot be represented reliably by inserting an “effective temperature” into every thermal-escape formula.

A6. Jeans Escape Flux — Full Derivation

Start with an isotropic Maxwellian at a conventional exobase. The upward number flux is the velocity-space integral of v_z f over particles with v_z > 0 and total speed v > v_{es}c:

$$\Phi_J = \int_(v>v_{es}c,\ v_z>0)\ v_z\ f_M\ d^3v \quad (A17)$$

Use spherical velocity coordinates with v_z = v cosθ and $d^3v = v^2 \sin\theta\ dv\ d\theta\ d\varphi$. Over the upward hemisphere, 0 ≤ θ ≤ π/2 and 0 ≤ φ < 2π:

$$\Phi_J = 2\pi n(m/2\pi kT)\^(3/2) \int_(v_{es}c)\^\infty v^3 e\^(-av^2)dv \int_0\^(\pi/2)\cos\theta \sin\theta\ d\theta \quad (A18)$$

The angular integral is 1/2. With x = av² and a = m/(2kT), the speed integral becomes:

$$\int_(v_{es}c)\^\infty v^3 e\^(-av^2)dv = [1/(2a^2)](1 + av_{es}c^2)e\^(-av_{es}c^2) \quad (A19)$$

Since $av_{es}c^2 = \lambda$ and $v_{mp} = 1/\sqrt{a}$:

$$\Phi_J = (n\ v_{mp}/2\sqrt{\pi})(1 + \lambda)e\^(-\lambda) \quad (A20)$$

This derivation assumes a locally isotropic Maxwellian and a lower atmosphere capable of refilling the loss cone. At the Moon, the solid surface emits only into the outward half-space, particles can stick on return, and the source may be nonthermal. Equation A20 is therefore a benchmark, not a complete lunar escape model.

A7. Chamberlain Exosphere Formalism

Step 1: Liouville’s theorem

In a stationary collisionless gravitational field, the phase-space density is constant along a trajectory: df/dt = 0. Suppose the populated trajectories originate at a reference level r_0 with a Maxwellian energy dependence. Conservation of specific energy gives:

$$v_0^2 = v^2 + 2\mu(1/r_0 - 1/r) \quad (A21)$$

Substituting this into the reference Maxwellian produces:

$$f(r,v) = C\ \exp[\lambda(r) - \lambda_0]\ \exp[-mv^2/(2kT)] \quad (A22)$$

If every velocity at r were populated, integrating equation A22 over all velocity space would recover the spherical barometric factor in equation A7. In a collisionless exosphere, however, not every local velocity corresponds to a trajectory connected to the source boundary.

Step 2: divide velocity space into trajectory classes

- Ballistic: bound trajectories that intersect the lower boundary and return to it.
- Escaping: unbound trajectories, $\mathcal{E} \geq 0$, on the outward branch supplied from below.
- Satellite: bound trajectories whose periapsis remains above the lower boundary.

For each class i, define a dimensionless partition function as the fraction of the full local Maxwellian contained in its allowed velocity-space domain D_i(r):

$$\zeta_i(r) = [\int_(D_i)\ \exp(-mv^2/2kT)d^3v] \ /\ [\int_(\text{all } v)\ \exp(-mv^2/2kT)d^3v] \quad (A23)$$

Let Z(r) = ζ_bal + ζ_esc + ζ_sat. The density is then:

$$n(r) = n(r_0)\ \exp[\lambda(r) - \lambda_0]\ Z(r)/Z(r_0) \quad (A24)$$

Equation A24 is the normalized Chamberlain density relation. It shows why the expression n = ñζ_bal e^(ε−ε̃) is incomplete: it omits the reference normalization and other possible trajectory classes, and it does not define whether ñ is a measured density or a full-Maxwellian normalization.

Lunar interpretation

A native thermal population launched from the solid lunar surface naturally fills ballistic trajectories and may fill an escaping component. It does not normally fill satellite trajectories, because those orbits never touch the source surface; thus ζ_sat is generally set to zero unless collisions, external injection, or time-dependent forces populate them. Surface roughness, adsorption, radiation pressure, photoionization, and nonthermal launch distributions are more naturally handled with Monte Carlo trajectory models, although the Chamberlain partition concept remains an essential analytic reference.

Why density can differ from a simple exponential

Near the surface, inaccessible directions, roughness, and non-Maxwellian low-speed populations can produce a ground-hugging component. At high altitude, escaping and radiation-pressure-accelerated particles can dominate. A single fitted scale height therefore need not correspond to a true temperature.

A8. Hodges–Johnson n_sT_s^(5/2) Relation

Physical assumptions

- The species is noncondensable and has negligible surface residence compared with flight time.
- Every surface encounter fully accommodates the particle to the local surface temperature T_s.
- There are no net local sources, losses, escape, ionization, or chemical conversion.
- Temperature varies slowly over a typical hop, gravity is locally constant, and ballistic transport can be expanded as a diffusion process.
- The surface is smooth enough that the Maxwell–Boltzmann-flux launch law applies.

Step 1: thermal hop moments

For the flux distribution, the horizontal components remain Gaussian with ⟨v_h²⟩ = 2kT/m. The upward component has p(v_z) = (m/kT)v_z exp[−mv_z²/(2kT)], giving:

$$\langle v_z\rangle = \sqrt{(\pi/2)}\sqrt{(kT/m)},\ \ \langle v_z^2\rangle = 2kT/m \quad (A25)$$

Using equations A11 and A13:

$$\langle \tau\rangle = \sqrt{(2\pi kT/m)/g} \quad (A26)$$

$$\langle L^2\rangle = 16(kT/m)^2/g^2 \quad (A27)$$

For an isotropic two-dimensional random walk, D_b = ⟨L²⟩/(4⟨τ⟩), so:

$$D_b = (2\sqrt{2}/\sqrt{\pi})(kT/m)\text{^}(3/2)/g \propto T\text{^}(3/2) \quad (A28)$$

Step 2: relate surface density to the mobile column

For a locally exponential thermal population, the column number per unit area is approximately:

$$N = \int_0\text{^}\infty n(z)dz = n_sH = n_skT/(mg) \propto n_sT \quad (A29)$$

Step 3: stationary state of a position-dependent random walk

When hop variance and hop rate are set by the temperature at the departure point, the diffusion-limit master equation has the form ∂N/∂t = ∇ₛ²(D_bN). The corresponding flux is J = −∇ₛ(D_bN). Zero net lateral flux therefore requires D_bN = constant. Combining equations A28 and A29:

$$D_{bN} \propto T^{(3/2)}(n_s T) = n_s T^{(5/2)} = \text{constant} \quad (A30)$$

$$n_s \propto T_s^{(-5/2)} \quad (A31)$$

A day/night temperature ratio of 400/100 = 4 therefore predicts n_night/n_day = 4^(5/2) = 32 for the ideal noncondensable equilibrium. This explains why He and Ne can have nightside maxima without condensing.

Why the law is approximate

Finite escape, photoionization, time-varying solar-wind supply, partial accommodation, surface residence, curvature, topography, roughness, and temperature changes across one long hop all alter the relation. If a surface residence time τ_{res} dominates the cycle time, D is reduced and no longer scales simply as T^(3/2). The law is therefore a valuable null model, not a universal constraint on every species.

A9. Surface Residence and Thermal Desorption

For first-order thermal desorption from a site with binding energy E_b and attempt frequency ν_0, the desorption rate and mean residence time are:

$$k_{des} = \nu_0 e^{(-E_b/kT)}, \quad \tau_{res} = \nu_0^{-1} e^{(E_b/kT)} \quad (A32)$$

Because T appears in the denominator of an exponential, small temperature changes can change residence time by many orders of magnitude. Real regolith has a distribution of E_b and site geometries, so one Arrhenius time is usually only an effective approximation.

A10. Pressure and Temperature in a Collisionless Population

The rigorous kinetic pressure is a tensor:

$$P_{ij} = m\int (v_i - u_i)(v_j - u_j) f \, d^3v \quad (A33)$$

Only for an isotropic Maxwellian does $P_{ij} = nkT\,\delta_{ij}$ and the scalar relation p = nkT apply. A sputtered or beam-like population can have different radial and tangential temperatures, and a fitted “effective temperature” may merely summarize a line-of-sight or altitude distribution.

A11. Radiation Pressure on Resonant Atoms

For a neutral atom with frequency-dependent absorption cross section σ_ν in spectral energy flux F_ν, the acceleration along the photon direction is:

$$a_{rad} = (1/mc)\int \sigma_\nu F_\nu \, d\nu \quad (A34)$$

For Na and K, resonance scattering makes this acceleration important. Because the solar line profile is sampled at a Doppler-shifted frequency, a_rad depends on the atom’s heliocentric radial velocity; it is not generally a single constant.

A12. Practical Model-Selection Guide

- Use H = kT/(mg) only as a local thermal scale and check H/r.
- Use constant-g hop equations only for short hops over locally flat terrain.
- Use Jeans escape only for a specified thermal distribution and clearly defined boundary density.
- Use Chamberlain partitions for analytic spherical collisionless populations connected to a lower boundary.
- Use Hodges–Johnson as a null model for noncondensable, fully accommodated, source-free lateral equilibrium.
- Use Monte Carlo or direct trajectory integration when sources are nonthermal, the surface is rough or temperature varies strongly, radiation pressure matters, or sticking/ionization occurs along the path.

JOINT AI/HUMAN AUTHORSHIP AND USE DISCLAIMER

AI Authorship and Review. This textbook was written and assembled using artificial intelligence systems, specifically ChatGPT 5.6 Sol and Grok 4.5, along with human writing by E.C. Joy. During its development, the book was built, checked, and revised through twenty-nine AI-assisted iterations involving two different AI systems. These iterations included reviews of factual accuracy, formatting, organization, and overall content. Human review, editing, selection, and modification were also performed moderately by E.C. Joy.

Limitations of Artificial Intelligence. Repeated review by artificial intelligence does not guarantee that every statement, equation, interpretation, citation, or numerical value is complete or correct. Artificial intelligence systems can produce inaccurate, incomplete, outdated, misleading, or fabricated information and may fail to identify errors introduced by another artificial intelligence system.

Intended Use. This book is intended solely as a general guide to lunar atmospheric science. It should not be used as a substitute for peer-reviewed literature, primary scientific sources, mission documentation, authoritative datasets, or qualified expert analysis. It should not be relied upon for in-depth scientific research, formal academic work, mission planning, professional decision-making, or safety-critical applications without independent verification. It should be treated in the same general manner as information encountered through Wikipedia, broad Google searches, or direct AI-generated responses: as a starting point for further investigation rather than as direct academic research.

Verification and Research Cutoff. Readers should independently verify important claims, equations, numerical values, and citations against current primary literature and authoritative scientific archives. This edition contains research and sources available through August 2026. Later discoveries, corrections, or revisions may not be reflected.

© 2026 E.C. Joy